Pergamon

www.neuroscience-ibro.com

PII: S0306-4522(02)00048-9

Neuroscience Vol. 112, No. 3, pp. 731–749, 2002
Published by Elsevier Science Ltd on behalf of IBRO
Printed in Great Britain
0306-4522/02 $22.00+0.00

INTRACEREBROVENTRICULAR BUT NOT INTRAVENOUS INTERLEUKIN-1β INDUCES WIDESPREAD VASCULAR-MEDIATED LEUKOCYTE INFILTRATION AND IMMUNE SIGNAL mRNA EXPRESSION FOLLOWED BY BRAIN-WIDE GLIAL ACTIVATION

M. G. PROESCHOLDT,[1] S. CHAKRAVARTY, J. A. FOSTER, S. B. FOTI, E. M. BRILEY and M. HERKENHAM*

Section on Functional Neuroanatomy, National Institute of Mental Health, Building 36, Room 2D15, Bethesda, MD 20892-4070, USA

Abstract—Interleukin-1β (IL-1β) is a pro-inflammatory cytokine that appears in brain and cerebrospinal fluid following peripheral immune challenges and central infections or injury. We examined the consequences of i.c.v. infusion of IL-1β on mRNA expression of several immune markers and on recruitment of peripheral leukocytes. Awake rats were infused with IL-1β (100 ng/rat) into the lateral ventricle, and 0.5, 2, 4, 8, 12, or 24 h later, animals were killed and their fresh-frozen brains processed for *in situ* hybridization and immunohistochemistry. Widespread vascular expression of inhibitory factor κBα (IκBα, marker of nuclear factor κBα transcriptional activity) and inducible cyclooxygenase (COX-2) mRNAs at 0.5–2 h was credited to movement of IL-1β along ventricular, subarachnoid, and perivascular pathways to target endothelia that express type 1 IL-1 receptor mRNA. Induction of monocyte chemoattractant protein-1 mRNA and intercellular adhesion molecule-1 (ICAM-1) immunostaining on endothelia began at 0.5–2 h. Leukocytes (neutrophils and monocytes, recognized by morphology and CD45 and ED1 immunostaining) appeared in meninges and blood vessels at 2–4 h and diffusely penetrated the parenchyma at 8–24 h. The leukocytes strongly expressed IL-1β and inducible nitric oxide synthase mRNAs. Beginning at 4–12 h, astrocytes (glial acidic fibrillary protein mRNA and protein and c-fos mRNA) and microglia (ionized calcium-binding adaptor molecule 1 mRNA and protein) showed widespread activation. Other rats received i.v. IL-1β (6 μg/kg). Their brains showed induction of IκBα and COX-2 mRNAs in the vasculature at 2 h but none of the other sequelae.

In summary, our data indicate that IL-1β in the cerebrospinal fluid reaches its target receptors on the endothelia via perivascular volume transmission, up-regulates ICAM-1, and triggers a targeted leukocyte emigration and widespread glial activation stimulated perhaps by pro-inflammatory molecules expressed by leukocytes. The dramatic difference between i.c.v. and i.v. routes of administration underscores the potency of IL-1β within the brain to dynamically affect the cellular trafficking component of 'immune privilege'. Published by Elsevier Science Ltd on behalf of IBRO.

Key words: nuclear factor κB, meningitis, astrocytosis, cyclooxygenase-2, intercellular adhesion molecule-1, monocyte chemoattractant protein-1, cerebrospinal fluid.

The potent pro-inflammatory cytokine interleukin-1β (IL-1β) plays a key role in immune regulation. Its induction in the CNS has been detected following peripheral (Buttini and Boddeke, 1995; Van Dam et al., 1995; Quan et al., 1998; Konsman et al., 1999) and central (Stern et al., 2000) immune challenge by endotoxin and following brain infection (Mustafa et al., 1989; Griffin, 1997; Plata-Salaman et al., 1999; Quan et al., 1999a), injury (Touzani et al., 1999; Herx et al., 2000), and neurodegenerative disease (Mrak and Griffin, 2000). Peripheral administration of the bacterial endotoxin lipopolysaccharide (LPS) results in the rapid (at 2 h) induction of IL-1β mRNA and protein in choroid plexus, circumventricular organs, vasculature, and meninges (Quan et al., 1998; Eriksson et al., 2000; Garabedian et al., 2000). Biologically active IL-1β is found in the cerebrospinal fluid (CSF) following either peripheral or central injection of LPS (Quan et al., 1994). IL-1β can potentially interact with IL-1 receptor bearing target cells (Ericsson et al., 1995) to activate the nuclear factor κB (NF-κB) transcription factor-mediated pathways that lead to induction of cytokines, prostaglandin E_2, and nitric oxide (Pahl, 1999) which have further consequences on cell function and animal physiology.

[1] Present address: Bezirksklinikum, Universitätsstrasse 84, 93053 Regensburg, Germany.

*Corresponding author. Tel.: +1-301-496-8287; fax: +1-301-402-2200.

E-mail address: milesh@codon.nih.gov (M. Herkenham).

Abbreviations: CSF, cerebrospinal fluid; COX-2, cyclooxygenase-2; GFAP, glial acidic fibrillary protein; Iba1 (or iba1), ionized calcium-binding adaptor molecule 1; ICAM-1, intercellular adhesion molecule-1; IκBα, inhibitory factor κBα; (rr)IL-1β, (rat recombinant) interleukin-1β; IL-1ra, IL-1 receptor antagonist; IL-1R1, type 1 IL-1 receptor; iNOS, inducible nitric oxide synthase; LPS, lipopolysaccharide; MCP-1, monocyte chemoattractant protein-1; NeuN, neuronal nuclei; NF-κB, nuclear factor κB; OVLT, vascular organ of the lamina terminalis; PBS, phosphate-buffered saline; PVN, paraventricular nucleus of the hypothalamus; SFO, subfornical organ; SSC, saline sodium citrate; TNF-α, tumor necrosis factor-α.

The hypothesis that the CSF plays an important role in conveying immune signals throughout the brain is supported by the observation that i.c.v. application of IL-1β elicits acute phase responses that are similar to those observed after peripheral immune challenge (Rothwell, 1991; Anforth et al., 1998). The flow of molecules in the CSF has recently been mapped in detail (Proescholdt et al., 2000). The rapid dissemination of the tracer molecule [^{14}C]inulin in the ventricular, subarachnoid (cisternal), and perivascular spaces is followed by a slower diffusion from the ventricles and cisternae into the brain parenchyma. This same pattern is reflected in the distribution of induced immune signal molecules following i.c.v. administration of IL-1β (Konsman et al., 2000) and tumor necrosis factor-α (TNF-α) (Nadeau and Rivest, 2000).

Another consequence of i.c.v. IL-1β administration is a CSF pleocytosis that has been proposed to be a model of bacterial meningitis (Ramilo et al., 1990; Quagliarello et al., 1991). Although it is known that i.c.v. IL-1β can induce leukocyte extravasation into the subarachnoid spaces, the relationship between the initial events and the appearance of leukocytes in the CSF is only partly understood. It is also not clear whether i.v. IL-1β can induce a similar series of events. The present study was designed to determine the spatiotemporal relationship between i.c.v. IL-1β administration and the appearance of induced immune signal molecules and leukocytes in the brain of awake rats. We also compared the responses to i.c.v. and i.v. IL-1β administration. The use of multiple markers across a broad time scale permits hypotheses to be tested about the molecular mechanisms that determine the cellular and physiological outcomes. Thus, the study used *in situ* hybridization histochemistry of mRNAs for inhibitory factor κBα (IκBα), IL-1β, TNF-α, cyclooxygenase-2 (COX-2), inducible nitric oxide synthase (iNOS), and several additional immune signal molecules. IκBα is a marker of NF-κB activity (Quan et al., 1997), IL-1β and TNF-α are potent pro-inflammatory cytokines, COX-2 (inducible COX) is a marker of prostaglandin E_2 production (Cao et al., 1999), and iNOS is a marker of nitric oxide production (Wong et al., 1996) under these circumstances. In addition, recruitment of a peripheral cellular response was assessed by *in situ* hybridization of the chemokine monocyte chemoattractant protein-1 (MCP-1) (Rollins, 1996) and immunohistochemistry of intercellular adhesion molecule-1 (ICAM-1), an adhesion molecule that promotes leukocyte adherence to vascular endothelia and diapedesis following IL-1β stimulation (Greenwood et al., 1995), and CD45 – leukocyte common antigen – a pan marker for white blood cells. Activation of astrocytes and microglia was assessed using cRNA probes and antibodies to glial acidic fibrillary protein (GFAP) and ionized calcium-binding adaptor molecule 1 (iba1), respectively. GFAP is a marker for astrocytes and astrocyte activation. Iba1 protein and iba1 message are microglia-specific molecules that show up-regulation in brain injury models (Imai et al., 1996; Ito et al., 1998). Finally, c-fos mRNA was used to show both neural and glial activation across the time course of the study.

EXPERIMENTAL PROCEDURES

Animals and procedures

Male Sprague–Dawley rats (242 ± 17 g at time of i.c.v. injection; Taconic Farms, Germantown, NY, USA) were used. Animals were housed in pathogen-free standard facility conditions with lights on from 06:00 to 18:00 h and *ad libitum* access to food and water. Animal procedures were approved by the National Institute of Mental Health Intramural Research Program Animal Care and Use Committee. All efforts were made to minimize the number of animals and their suffering. After acclimatization, animals were anesthetized with isoflurane and placed in a stereotaxic apparatus (Kopf Instruments, Tujunga, CA, USA). Stainless steel cannulae (26 gauge; Plastics One, Roanoke, VA, USA) were implanted into the right lateral ventricle at 0.6 mm posterior and 1.3 mm lateral to bregma (final depth: 4.3 mm from skull). After correct positioning, cannulae were fixed to the skull with screws and cranioplastic cement and sealed with 33-gauge dummy cannulae (Plastics One). Animals were housed singly thereafter. They were given subcutaneous fluids for the first 3 post-operative days, and their diets were supplemented.

Following a recovery period of 10–18 days, animals received either 100 ng in 5 μl of recombinant rat IL-1β (rrIL-1β) ($n = 5$ per time point) or 5 μl of carrier solution ($n = 2$ per time point) delivered at a constant rate over 2 min by a microinjection pump (Stoelting, Wood Dale, IL, USA). rrIL-1β (R&D Systems, Minneapolis, MN, USA; cat #501-RL) was dissolved in sterile phosphate-buffered saline (PBS) containing 0.1% rat serum albumin (Sigma, St. Louis, MO, USA). Control animals received PBS+albumin (vehicle) only. All solutions were prepared fresh and held at 4°C. rrIL-1β or vehicle was infused into awake, freely moving animals using a 33-gauge injection cannula (Plastics One) connected to PE-50 tubing and a 100-μl Hamilton syringe. The injection cannula protruded slightly beyond the guide cannula. Animals were killed by decapitation 0.5, 2, 4, 8, 12, or 24 h later. Following quick removal, brains were frozen in 2-methyl butane on dry ice and stored at −70°C. To assure minimal interactions with endogenous corticosterone levels, injections were performed either early in the morning (0.5-, 2-, 4-, and 24-h time points) or late at night (8- and 12-h time points), and all animals were killed before noon.

A second set of rats ($n = 15$; same source) was prepared for i.v. rrIL-1β administration. Sterile silastic catheters (Baxter Healthcare, McGaw Park, IL, USA) were implanted in the external jugular vein as described previously (Herkenham et al., 1998), with the plugged catheters exiting from the back between the scapulae. Two days later, awake rats received i.v. IL-1β (6 μg/kg; same source as above) or vehicle (sterile 0.9% saline) and were killed 2 or 12 h later, all in the morning. The dose was selected to ensure a brain response, in the form of mRNA induction, in addition to fever. $n = 5$ for each experimental group, and $n = 3$ and 2 for the 2- and 12-h control groups, respectively.

Histology

Cryostat-cut 15-μm-thick slide-mounted coronal sections were further processed for *in situ* hybridization histochemistry and immunohistochemistry. Sections were collected in a spaced series from the frontal pole through the caudal medulla, with concentration at the cannula track, vascular organ of the lamina terminalis (OVLT), subfornical organ (SFO), hypothalamic paraventricular nucleus (PVN), central nucleus of amygdala/median eminence, pituitary, locus coeruleus, and area postrema. Slides were stored at −35°C until further processing.

The *in situ* hybridization procedures were performed as described previously for ribonucleotide (cRNA) probes (Stern et al., 2000). First, tissue sections were processed by fixation with 4% formaldehyde solution, acetylation with 0.25% acetic anhydride in 0.1 M triethanolamine–HCl, pH 8.0 solution, dehydration with ethanol, and delipidation with chloroform.

Second, the antisense probes were transcribed using the Riboprobe System (Promega Biotech, Madison, WI, USA) with [α-^{35}S]UTP (specific activity >1000 Ci/mmol; New England Nuclear, Boston, MA, USA) and T7, T3, or SP6 RNA polymerase. The applied rat cRNA probes consisted of IκBα (gift of Dr. Rebecca Taub, University of Pennsylvania, Philadelphia, PA, USA), c-fos (gift of T. Curran, Roche Institute of Molecular Biology, Nutley, NJ, USA), IL-1β (a 498-bp *Eco*RI/*Xba*I fragment acquired from Dr. Ronald Hart, Rutgers University, Newark, NJ, USA, subcloned into a pBluescript SK+ vector), type 1 IL-1 receptor (IL-1R1) and IL-1 receptor antagonist (IL-1ra) (plasmids generously provided by Dr. Hart), TNF-α (gift from Dr. Karl Decker, Albert-Ludwigs Universität, Freiburg, Germany), iNOS (gift from Dr. Elena Galea, Cornell Medical Center, New York, NY, USA), COX-2 (gift of Dr. Daniel Hwang, Pennington Biomedical Research Center, LA State University, Baton Rouge, LA, USA), GFAP (gift of Dr. D. Feinstein, Cornell University School of Medicine, New York, NY, USA), iba1 (gift of Dr. Yoshori Imai, National Institute of Neuroscience, Tokyo, Japan), MCP-1 (gift of Dr. Jeffrey S. Warren, University of Michigan Medical School, Ann Arbor, MI, USA), and CD14 (full-length mouse cDNA generated by polymerase chain reaction and subcloned into a pGEM-TEasy vector by Dr. Sumana Chakravarty in this laboratory).

The radiolabeled probes were diluted in a riboprobe hybridization buffer and applied to brain sections (approximately 500 000 c.p.m./section). After overnight incubation at 55°C in a humidified chamber, slides containing brain sections were washed first in 20 μg/ml RNase solution and then 1 h each in 2× saline sodium citrate (SSC; 50°C) and 0.2× SSC (55 and 60°C) solutions to reduce non-specific binding of the probe. The slides were then dehydrated with ethanol and air-dried for autoradiography.

Slides and ^{14}C plastic standards containing known amounts of radioactivity (American Radiochemicals, St. Louis, MO, USA) were placed in X-ray cassettes, apposed to film (BioMax MR, Kodak, Rochester, NY, USA) for 2–13 days, and developed in an automatic processor (X-OMAT, Kodak). Selected slides were dipped in nuclear track emulsion (NTB-2, Kodak), exposed for 1 month, developed (D-19, Kodak), and counterstained with Cresyl Violet.

Immunohistochemistry was performed on other sets of the slide-mounted sections. Monoclonal antibodies used were mouse anti-rat CD45 (leukocyte common antigen; 1:500 dilution; Serotec, Oxford, UK), ED1 (1:500 dilution; Serotec), CD3 (1:500 dilution; Serotec), or CD54 (ICAM-1; 1:500 dilution; Serotec). Slides were brought to room temperature and fixed in Histochoice (Amnesco, Solon, OH, USA) for 12 min, washed in 1× PBS, pH 7.4, incubated in methyl alcohol containing 0.5% hydrogen peroxide for 20 min, washed in 1× PBS, and incubated in blocking reagent containing 1× PBS, 2% bovine serum albumin (Sigma), and 2% normal horse serum (Vector Laboratories, Burlingame, CA, USA) for 1 h. Thereafter, slides were incubated with the respective primary antibodies overnight at 4°C. After additional washes in 1× PBS, slides were incubated with biotinylated secondary anti-mouse antibody (1:200 dilution; Vector) for 45 min, washed in 1× PBS, then incubated with avidin–biotin (Vector) reagent for 30 min and again washed in 1× PBS. The chromogen reaction was developed by incubating slides with 3,3′-diaminobenzidine in the presence of hydrogen peroxide (Vector). Polyclonal antibodies used were rabbit anti-cow GFAP (1:4000 dilution; Dako, Carpinteria, CA, USA) and rabbit anti-rat Iba1 (1:500 dilution; gift of Dr. Yoshinori Imai, National Institute of Neuroscience, Tokyo, Japan). Slides were treated as above except they were fixed in 4% paraformaldehyde in 1× PBS for 12 min, washed in 1× PBS, and incubated in blocking reagent containing 2% normal goat serum (Vector) for 1 h. Thereafter, slides were incubated with the primary antibodies as above, quenched in methyl alcohol containing 0.5% hydrogen peroxide for 20 min, washed, incubated with biotinylated secondary anti-rabbit antibody (1:200 dilution, Vector), and processed as above.

Some sections were processed for double-label *in situ* hybridization and immunohistochemistry, using ^{35}S-labeled c-fos mRNA and mouse anti-neuronal nuclei (NeuN) monoclonal primary antibody (Chemicon, Temecula, CA, USA). The hybridization procedure was applied first, as described above, followed by the described immunohistochemistry. Additional double-label *in situ* hybridization procedures combined digoxigenin-labeled GFAP cRNA with ^{35}S-labeled c-fos cRNA. Here the two probes were hybridized simultaneously as previously described (Hohmann and Herkenham, 1999). After all double-label procedures, slides were emulsion-coated in LM-1 (Amersham, Piscataway, NJ, USA).

In some sections, dual fluorescent immunohistochemistry was used to detect CD45-labeled leukocytes in combination with lectin staining for blood vessels. The primary antibody for CD45 was applied as above, followed by 5 μg/ml Cy3-labeled anti-mouse IgG (Jackson ImmunoResearch Laboratories, West Grove, PA, USA) and 10 μg/ml Alexa 488-conjugated Lectin HPA (Molecular Probes, Eugene, OR, USA).

Autoradiographic film images were digitized with a solid-state camera (CCD-72, Dage-MTI) and a Macintosh computer using NIH Image software (Wayne Rasband, National Institute of Mental Health). Illustrations were made directly from these images. All images were contrast-enhanced identically in the composites. Densitometry was performed on images at the PVN level. Mouse cursor control was used to outline the right and left somatosensory cortex, corpus callosum, caudate–putamen, internal capsule, thalamus, PVN, hypothalamus, and meninges at the base of the brain. Transmittance measurements were converted to d.p.m./mg plastic using a calibration curve generated from the standards. Background transmittance was not subtracted from the density calculations. Group density means were calculated for each structure, but because of the small number of animals in the control groups at each time point, statistics were not performed. However, assignments of peak levels of induction and right–left differences were based on the quantitative measurements.

Microphotography through a Leica DMR microscope was done with digital camera (Sensys 1600 or CoolSnap cf, Photometrics, Tucson, AZ, USA) and IPLab Spectrum software (Scanalytics, Fairfax, VA, USA). Fluorescent images were captured using SlideBook software (Intelligent Imaging Innovations, Denver, CO, USA). All images were processed in Adobe Photoshop (Adobe software) using the Levels, Filter, and Contrast features to optimize them.

RESULTS

Rats given injections of 100 ng IL-1β into the lateral ventricle showed variable signs of behavioral response to the cytokine – diarrhea, piloerection, and sleeping – beginning by about 0.5 h after the injection. Rats given vehicle showed no observable behavioral change. Rats given i.v. IL-1β (6 μg/kg) shuddered slightly and showed piloerection at the time of injection, then appeared normal. Both of the IL-1β doses by these routes of administration, as well as lower doses, have been shown to induce fever in rats (Dascombe et al., 1989), albeit with different formulations of IL-1β.

Table 1 shows the markers used in the experiment and the overall temporal patterns of their induction after i.c.v. IL-1β administration. Animals used in the following account were those that showed correct cannula placement, normal weight gain and behavior over the course of the experiment, and no gross histopathology. For each time point, three to five animals satisfied the criteria for inclusion, and they all showed the patterns of activation described.

Abbreviations used in the figures

AP	area postrema
Arc	arcuate nucleus
BLA	basolateral nucleus of amygdala
bv	blood vessel
CA1, CA3	Cornu ammonis fields of hippocampus
cc	corpus callosum
Ce	central nucleus of amygdala
Ch Plx	choroid plexus
cp	cerebral peduncle
CPu	caudate–putamen
DG	dentate gyrus
gl	glia limitans
Hb	habenula
hf	hippocampal fissure
ic	internal capsule
LH	lateral hypothalamus
LP	lateral posterior nucleus
LV	lateral ventricle
ME	median eminence
Men	meninges
MH	medial hypothalamus
opt	optic tract
ox	optic chiasm
RSG	granular retrosplenial cortex
SNR	substantia nigra pars reticulata
S1	primary somatosensory cortex
vhc	ventral hippocampal commissure
3V	third ventricle

Early mRNA induction patterns at 0.5–4 h after i.c.v. IL-1β

Following the i.c.v. infusion of IL-1β, several mRNAs showed induction at the 0.5-h time point. These were IκBα, c-fos, IL-1β, TNF-α and MCP-1. Beginning at 2 h, COX-2 mRNA was strongly induced. These early inductions were mainly associated with the brain vasculature.

IκBα mRNA. Following i.c.v. injection of vehicle, IκBα mRNA expression was induced slightly in the ventricular ependyma near the injection site, in the ipsilateral choroid plexus of the lateral ventricle, and in the basal meninges at 0.5 h (Fig. 1a–c). In contrast, following i.c.v. injection of IL-1β, widespread strong IκBα mRNA induction was seen throughout the brain's vasculature, meninges, choroid plexus, ependyma, and circumventricular organs. At 0.5 h, labeling appeared in these compartments throughout the entire brain (Fig. 1d–f). The vascular labeling within the brain parenchyma was fairly homogeneously distributed at 0.5 h, although the rostral thalamus and medial hypothalamus around the third ventricle had elevated labeling intensity (Fig. 1e, f).

The IκBα mRNA labeling subsequently became more completely distributed throughout the brain's microvasculature, although at later time points there was a less dense labeling in the contralateral striatum and adjacent deep cortical layers (Fig. 1g, h). IκBα mRNA expression

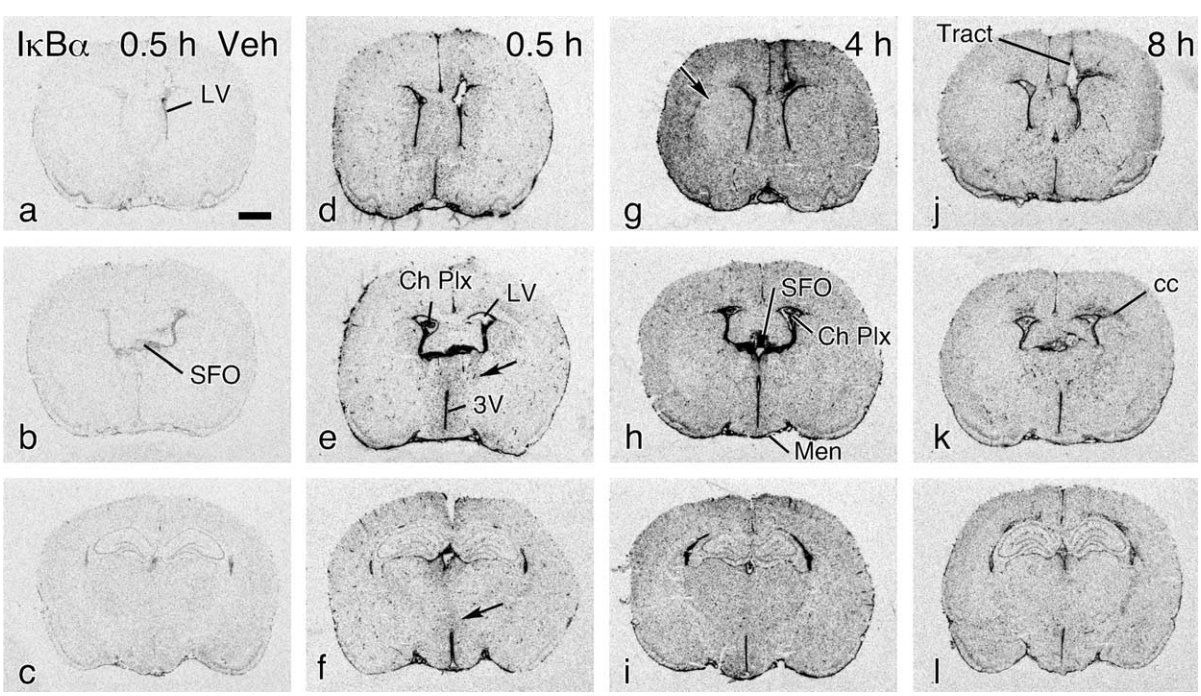

Fig. 1. Film images show IκBα mRNA expression of vehicle-injected animals at 2 h (a–c) and i.c.v. IL-1β-injected animals at 2 h (d–f), 4 h (g–i), and 8 h (j–l). Coronal levels of brain shown are the OVLT and/or cannula track, SFO, and posterior median eminence. The vehicle-induced IκBα mRNA expression (practically none) is shown in the first column (a–c). IL-1β-induced labeling is located in ventricular ependyma, meninges, choroid plexus, circumventricular organs, and blood vessels (see text). The arrows in e, f, and g point to locations where the IL-1β-induced labeling appears to reflect the expected pattern of spread of molecules introduced into the extracellular fluid compartment, based on the [^{14}C]inulin data (Proescholdt et al., 2000). Scale bar = 2 mm.

Table 1. Summary of cRNA probes and antibodies used and the salient features of their induced expression following i.c.v. IL-1β administration (100 ng in 5 μl infused into the right lateral ventricle over a 2-min period)

Name	Marker of	Predominant expressing cell type	Temporal induction pattern in h (peak)
c-fos	Transcriptional activation via AP-1	Neurons early; glia (astrocytes) late	0.5–2 (2); 0.5–12 (4–8)
TNF-α	Pro-inflammatory cytokine	Vascular/meninges	0.5–2 (2)
MCP-1	Monocyte chemoattraction	Endothelia	0.5–8 (2–4)
IκBα	Transcriptional activation via NF-κB	Endothelia, choroid plexus, ependyma, meninges, leukocytes	0.5–12 (4)
IL-1β	Pro-inflammatory cytokine	Meninges, ependyma, endothelia, leukocytes	0.5–12 (4–8)
COX-2	Prostaglandin E_2 synthesis	Endothelia	2–8 (4)
iNOS	Nitric oxide synthesis	Glia (early), leukocytes	2–12 (4–8)
ICAM-1 (CD54)	Cell adhesion molecule induction	Endothelia	2–24 (8–12)
CD45 (LCA)	Leukocyte common antigen; leukocytes (white blood cells)	Neutrophils, monocytes	4–24 (8–24)
ED1	Myeloid cell glycoprotein	Macrophages	4–24 (8–24)
CD3	T cell receptor complex	T lymphocytes	4–24 (8–12)
CD14	LPS receptor, TNF-α signaling	Meninges	4–12 (8)
IL-1R1	Type 1 IL-1 receptor	Endothelia, leukocytes	4–12 (8–12)
IL-1ra	Anti-inflammatory cytokine	Leukocytes, ependyma	4–12 (12)
GFAP	Astrocyte activation	Astrocytes	4–24 (12–24)
iba1	Microglial activation	Microglia, leukocytes	8–24 (24)

Markers are arranged in order of onset of significant appearance.

intensity peaked at 4 h (Fig. 1g–i), then declined at 8 h (Fig. 1j–l). In some animals, the ipsilateral corpus callosum showed elevated labeling at 8 h (Fig. 1j, k). Clearly identified populations of leukocytes (see below) were labeled.

c-fos mRNA. Many cell types distributed throughout the brain showed c-fos mRNA expression following i.c.v. IL-1β administration. An early discrete neuronal pattern of expression was replaced later by a widespread, mostly non-neuronal pattern. Vehicle-injected animals showed neuronal c-fos mRNA expression in many locations at 0.5 h, but this diffuse neuronal induction disappeared at later time points. Like vehicle-injected animals, IL-1β-injected animals showed early induction of c-fos mRNA in neuronal structures (data not shown). At 2 h, however, the widespread c-fos mRNA expression pattern declined dramatically in the control animals (Fig. 2a–c) but increased in the IL-1β-injected animals (Fig. 2d–f). The IL-1β-induced c-fos mRNA expression peaked at 4 h

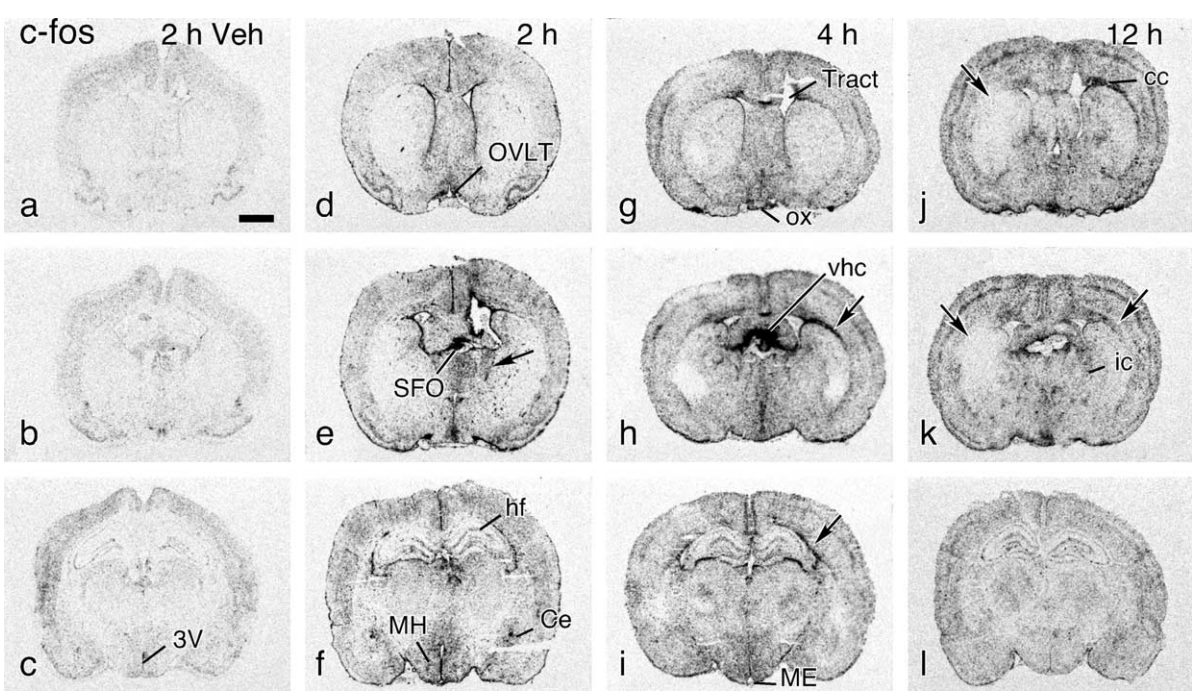

Fig. 2. Film images show c-fos mRNA expression in vehicle-injected (a–c) animals at 2 h and i.c.v. IL-1β-injected animals at 2 h (d–f), 4 h (g–i), and 12 h (j–l). Arrows point to elevated or low labeling associated with CSF flow pathways (e, j, k) and with reactive labeling increases in the ipsilateral corpus callosum and glia limitans surrounding the lateral ventricle (h, i, k). Scale bar = 2 mm.

(Fig. 2g–i). It declined gradually but was still present at 12 h (Fig. 2j–l).

The c-fos mRNA induction pattern at 2 h showed noteworthy density gradients suggestive of known CSF flow and diffusion patterns. At the levels of the OVLT and SFO, labeling appeared slightly more prominent ipsilaterally than contralaterally in the general region of the globus pallidus and the neocortex (Fig. 2d, e). At the level of the third ventricle and median eminence, c-fos mRNA labeling surrounded the third ventricle with a gradient of decreasing density (Fig. 2f).

The gradients of c-fos mRNA expression density disappeared by 4 h, at which time diffuse labeling was seen throughout most of the brain (Fig. 2g–i). Certain areas, such as that surrounding the SFO (Fig. 2h) and the glia limitans, remained especially elevated at 4 and 8 h. The ipsilateral corpus callosum in some but not all animals showed selectively elevated labeling intensity (Fig. 2h). An area of selectively sparse labeling continued to be the contralateral striatal/cortical region, seen in most animals (Fig. 2j, k).

IL-1β and IL-1R1 mRNA. Vehicle-injected animals showed no IL-1β mRNA expression (blank films, data not shown). Following i.c.v. IL-1β injection, the induction of IL-1β mRNA was widespread throughout the brain (Fig. 3). Compared to IκBα mRNA induction, the expression of IL-1β mRNA was temporally delayed and more restricted to the meninges and larger blood vessels. Expression was detectable at 0.5 h (Fig. 3a–d), and it consisted of labeled cells widely scattered in the meninges, ventricular ependyma, choroid plexus, and a few penetrating blood vessels. At 2 h, there was stronger expression in the same structures. At 4 h, ventricular expression was entirely gone, but greatly intensified expression levels were associated with the meninges (Fig. 3e–h). Labeling in the parenchyma was widespread and associated with the vasculature. At 8 h, discrete intense IL-1β mRNA expression was localized to the subarachnoid and perivascular spaces where leukocytes were accumulated (see below). A low level of parenchymal vascular-associated expression showed a regional elevation of density that matched the CSF flow pattern (arrows in Fig. 3i, j). Vascular labeling was notably absent in the contralateral striatal and cortical territory at 8 h (Fig. 3i, j). At 12 and 24 h, IL-1β mRNA expression levels greatly declined.

The pattern of mRNA distribution of the IL-1R1 is shown for comparison in the right-hand column of Fig. 3 (Fig. 3m–p). In agreement with the published pattern of

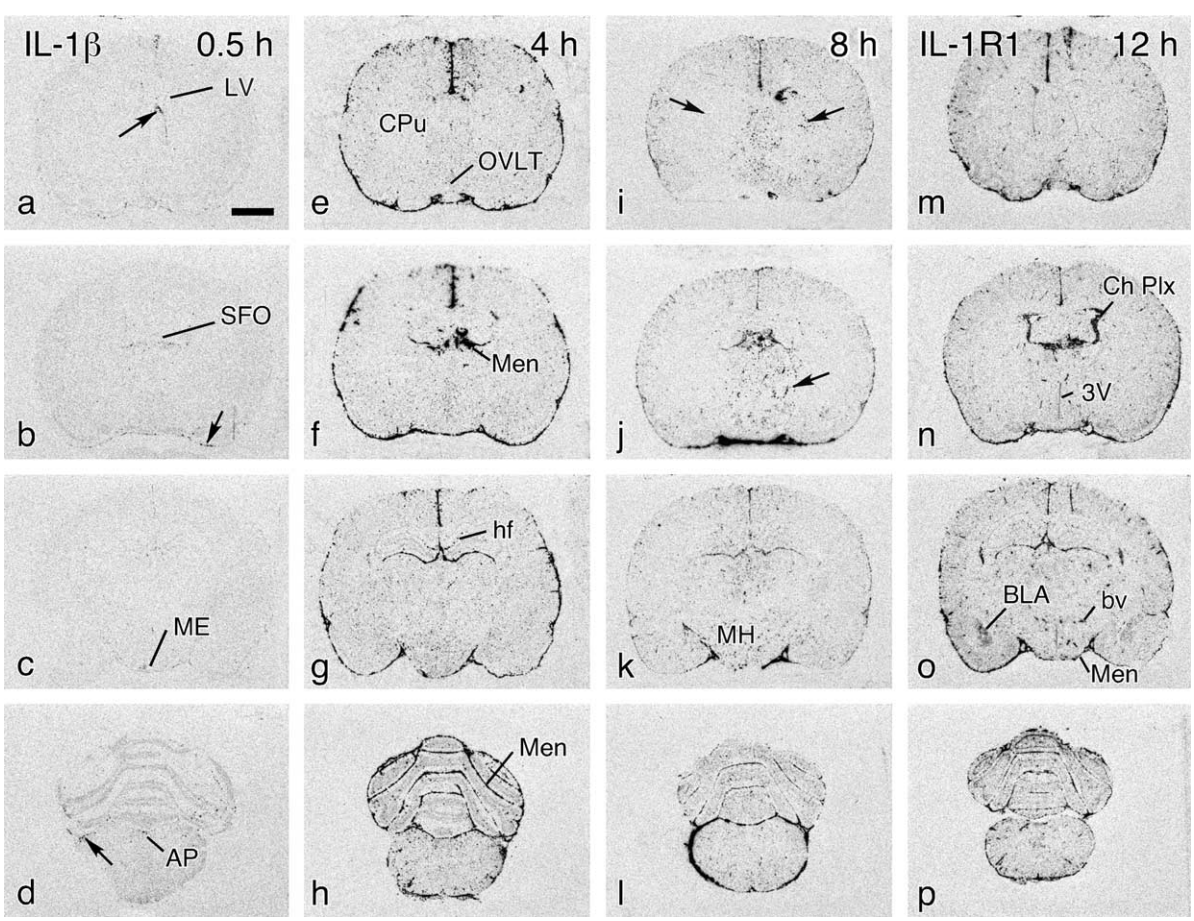

Fig. 3. Film images show IL-1β mRNA induction following i.c.v. IL-1β administration. Time points shown are 0.5 (a–d), 4 (e–h), and 8 h (i–l). Arrows point to labeled cells near the injection site (a) and in the meninges (b, d). The arrows in i and j point to locations where the densitometry indicated a significant group-wide difference in labeling density between right and left sides in these locations. The last column of images shows the mRNA expression pattern of the IL-1R1 at the same levels of brain (m–p). The time point shown is 12 h. Note induction of message along the cannula tract (m). Scale bar = 2 mm.

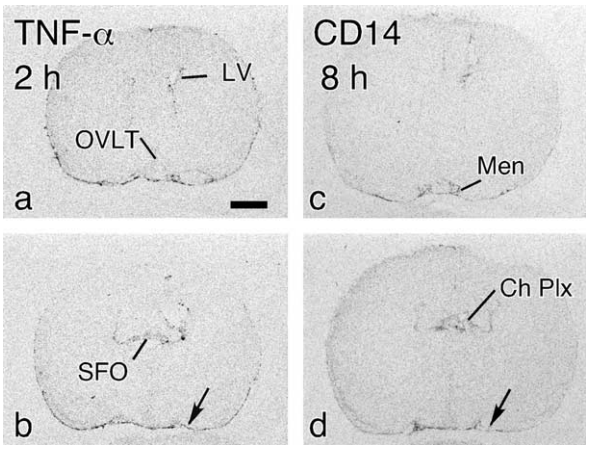

Fig. 4. Film images show TNF-α (a, b) and CD14 (c, d) mRNA induction following i.c.v. IL-1β administration. Time points selected illustrate peak levels of induction. Arrows point to sites of induction. Scale bar = 2 mm.

constitutive IL-1R1 mRNA distribution (Ericsson et al., 1995), widespread expression was seen in the meninges, choroid plexus, ventricular ependyma, and blood vessels. A complete time course was hybridized with the IL-1R1 riboprobe. Densitometry of the labeling, using the density slice feature to focus on the vascular and meningeal labeling, showed density increases above vehicle control levels beginning at 4 h and increasing over time to reach peak increases (approximately 300% of control in the meninges) at 12 h. Most or all of this increase was due to IL-1R1 mRNA expression by infiltrating leukocytes (see below).

TNF-α and CD14 mRNAs. Following i.c.v. IL-1β administration, barely detectable TNF-α mRNA induction was observed only at 0.5–2 h along the base of the brain and in the choroid plexus of the lateral ventricle (Fig. 4a, b). In the same locations, barely detectable CD14 mRNA induction was observed at 4–12 h (Fig. 4c, d). The same TNF-α and CD14 ribonucleotide probes strongly labeled parenchymal cells following intrastriatal LPS injection (Stern et al., 2000; Chakravarty and Herkenham, unpublished data).

COX-2 mRNA. After vehicle injection, COX-2 mRNA was expressed in the characteristic constitutive pattern, notably in neurons of the cerebral cortex and hippocampus. The pattern was not greatly changed at 0.5 h post-IL-1β injection (data not shown). At 2 h, a nearly exclusively vascular pattern of mRNA induction appeared (Fig. 5a) and reached peak levels at 4 h (Fig. 5b). The level of labeling dramatically declined at 8 h, at which time only scattered blood vessels and parts of the meninges were still labeled (Fig. 5c).

MCP-1 mRNA. Vehicle-injected animals showed no signal for MCP-1 mRNA expression at any location or time point (e.g. Fig. 5f). Induction of MCP-1 mRNA was clearly evident at 0.5 h after i.c.v. IL-1β (Fig. 5d). The choroid plexus was the most intensely labeled, but blood vessels and meninges at the base of the brain and in the parenchyma along the midline were also positive. At 2–4 h, labeling in these regions increased, parenchymal vascular expression was widespread, and labeling was seen also along the ventricular ependyma (Fig. 5e, f). The labeling decreased sharply by 8 h.

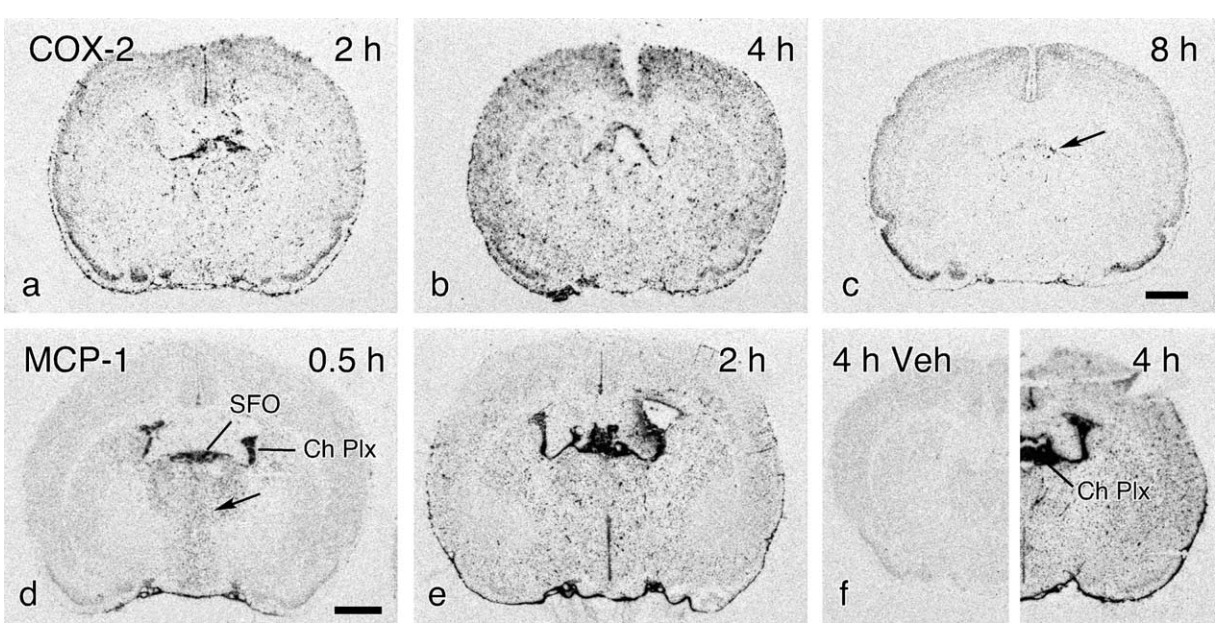

Fig. 5. Film images in a–c show COX-2 mRNA expression at the beginning (2 h; a), peak (4 h; b), and decline (8 h; c) of its induction in blood vessels following i.c.v. IL-1β administration. The cortical and hippocampal mRNA expression seen in isolation at 8 h is constitutive and neuronal. Arrow in c points to isolated blood vessels and meninges with induced COX-2 message. Film images in d–f show MCP-1 mRNA expression at the level of the SFO induced initially at 0.5 h (d) in the choroid plexus and meninges and along the diencephalic midline (arrow), then expanding to cover much of the brain's vasculature at 2 h (e) and 4 h (f, right) before declining to barely detectable levels. Vehicle-injected animal at 4 h is shown for comparison in f, left side. Scale bar = 2 mm.

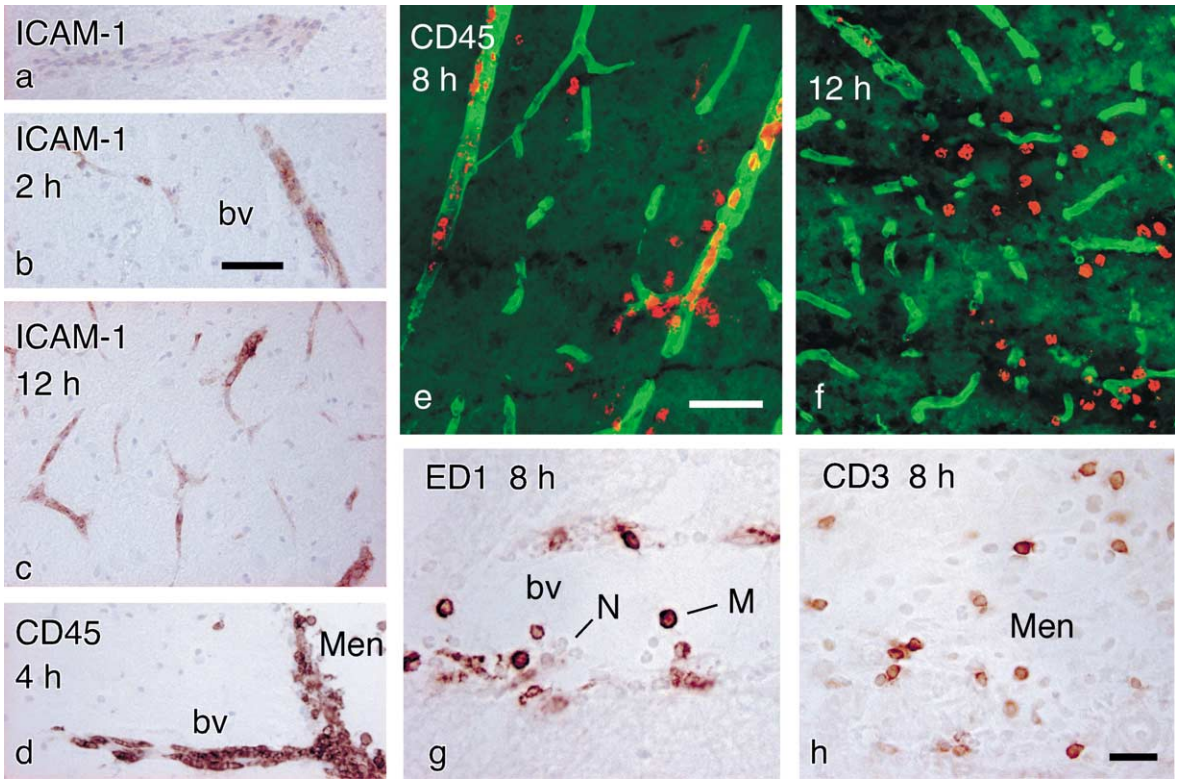

Fig. 6. Color photomicrographs show immunostaining for ICAM-1 (a–c), CD45 (d–f), ED1 (g), and CD3 (h) at several time points following i.c.v. vehicle (a) or IL-1β administration. The blood vessels stained for ICAM-1 (a–c) were located in the thalamus. In d, the meninges and blood vessels stained for CD45 were located in the rhinal sulcus. The pseudocolor images in e and f were taken with fluorescence illumination to show the relationship of the CD45-positive leukocytes (red) and brain blood vessels (green) in the superficial layers of the dorsolateral cerebral cortex. The large vessel stained for ED1 in g is located in the ventral mesencephalon. The CD3-positive lymphocytes in h are part of a cluster of leukocytes in the ambient cistern, between the medial geniculate nucleus and the hippocampus. Examples of immunostained monocyte/macrophages in g are marked M; unstained neutrophils are visible in high contrast and are marked N. Note that cells of both types are in several locations – within the lumen of the vessel, attached to the vessel wall, within the vessel wall, or just inside it. Scale bars = 50 μm (a–f) and 20 μm (g, h).

Late response patterns beginning prominently at 4 h after i.c.v. IL-1β

The late response pattern throughout the brain was associated closely with the up-regulation of the cell adhesion molecule ICAM-1 on blood vessels and the associated widespread appearance of infiltrating leukocytes that transiently expressed a number of immune signal mRNAs. Finally, astrocyte and microglial activation occurred, as will be described below.

ICAM-1 immunostaining. Immunostaining of ICAM-1 was strong in the choroid plexus of all animals, and it did not change in the IL-1β-injected animals (data not shown). Staining of the vasculature was only barely visible in control animals (Fig. 6a). Widespread induction of dark staining was seen at 2–4 h in the IL-1β-injected animals, when it was mostly confined to the larger vessels (Fig. 6b). At 8–12 h, smaller vessels and capillaries were stained (Fig. 6c). Elevated ICAM-1 immunostaining was still present at 24 h, though with less intensity in the small vessels.

CD45, ED1, and CD3 immunostaining. In vehicle-injected animals and animals 0.5 h post-IL-1β injection, scattered CD45-positive cells were found in the choroid plexus and more sparsely in the subarachnoid spaces (Fig. 7a). These cells were round, with fine, barely visible processes (Fig. 7a, inset). Increased numbers of positive cells were evident in the subarachnoid spaces and in the larger penetrating blood vessels at 2–4 h (Fig. 6d). Beginning at 8 h (Figs. 6e and 7b, d, e) and extending through the 24-h period examined, CD45-positive cells were more likely to be found scattered as individual cells throughout the neuropil. At 12 h, CD45-positive cells were clearly present in the neuropil (Fig. 6f). At 24 h, cells in large vessels were fewer, and isolated dispersed cells predominated (Fig. 7c).

The overall distribution of CD45-immunostained cells at the later time points was not homogeneous. An example is shown in Fig. 7d, where higher concentrations were found nearer to the cortical surface and especially in the cingulate and retrosplenial cortices adjacent to the longitudinal fissure. In addition, high concentrations of stained cells filled the hippocampal fissure, from which they appear to have invaded the medial parts of the dentate gyrus.

The ED1 antibody marked a subset of the CD45-immunostained cells (Fig. 6g). The two major populations of infiltrating blood leukocytes appearing in the brain

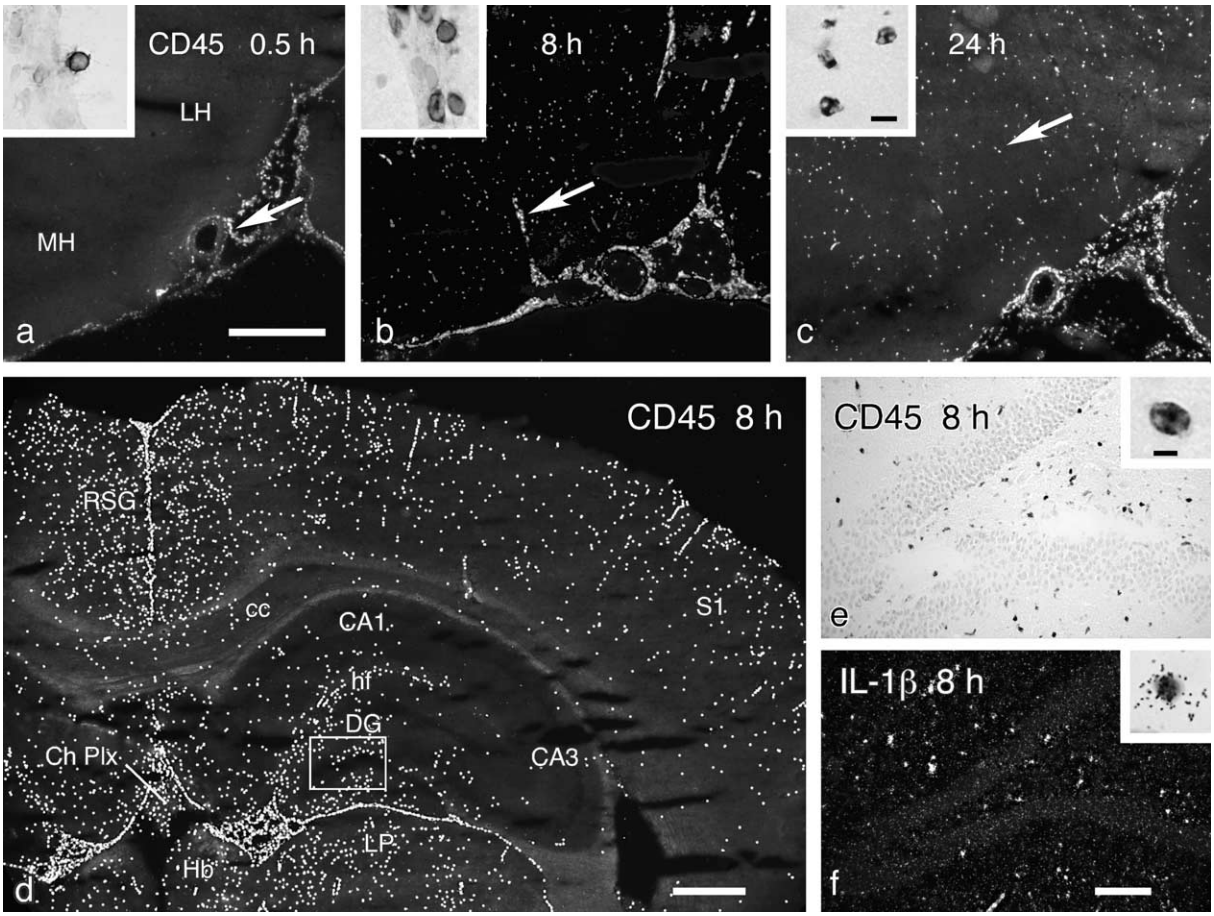

Fig. 7. Low-magnification dark-field photomicrographs in a–c show CD45 immunostaining at the level of the hypothalamus at 0.5 h (a), 8 h (b), and 24 h (c) following i.c.v. IL-1β administration. Insets show at high magnification what the immunostained leukocytes look like in the meninges (a), blood vessels (b), and parenchyma (c) at the respective time points. Arrows point to locations of inset illustrations. The level of the dorsal hippocampus and overlying cerebral cortex at the 8-h time point is shown in d–f. The low-magnification photograph in d but not the other panels was altered in Adobe Photoshop to make the CD45-positive cells more visible – each cell appearing as a white spot several pixels in diameter was individually enlarged using the paintbrush tool to about four times its size. The box in d shows the location of e, which is a bright-field photograph showing the individual immunoreactive cells concentrated in the dentate gyrus molecular layer and hilus. A nearby section hybridized for IL-1β mRNA is shown in f, dark-field illumination. Insets in e and f show individual labeled cells. Similar distribution patterns and cell sizes argue for the expression of IL-1β mRNA by the leukocytes. The cell in e, inset appears smaller than the cell in f, inset; this may be because the Nissl stain in this material shows only the cell nucleus, whereas the CD45 immunoreactivity is on the cell surface. Scale bars = 500 μm (a–d), 100 μm (e, f), 10 μm (inserts in a–c) and 5 μm (inserts in e, f).

after pro-inflammatory cytokine challenge are neutrophils and monocytes, and the ED1 antibody marked the monocyte/macrophage population preferentially. The smaller neutrophils could be recognized by their nuclear morphology. The major site of ED1-stained cells was the meninges and the larger blood vessels. There were many fewer ED1-positive cells seen in isolation throughout the brain parenchyma relative to CD45-positive cells, and those that were in the parenchyma appeared to be associated with blood vessels, suggesting that they had not transmigrated into the brain beyond a perivascular location.

The CD3 antibody marked the lymphocyte subset of the infiltrating leukocytes. These cells were rare, and they were only found in the subarachnoid spaces of the cisternae (Fig. 6h) and never in the parenchyma. They were present in the 4–24-h range, peaking at 8–12 h (Table 1). Thus, the major immune cell type to enter the parenchyma appears to be the neutrophil, based on immunostaining characteristics (CD45+, ED1−, CD3−).

iNOS mRNA. No clear expression of iNOS mRNA could be seen in vehicle-injected animals at any time point or in IL-1β-injected animals at 0.5 h. At 2 h after i.c.v. IL-1β injection, occasional iNOS mRNA-positive cells could be seen several locations immediately adjacent to the ependymal cells of the lateral and third ventricles. At later time points, the spatiotemporal induction pattern of iNOS mRNA closely matched that of IL-1β mRNA (compare Figs. 3 and 8). At 4 h, the meninges were strongly labeled (Fig. 8a). Meninges and blood vessels were labeled at 8 h (Fig. 8b) and declined thereafter. The patterns corresponded with the locations of the CD45-positive leukocytes.

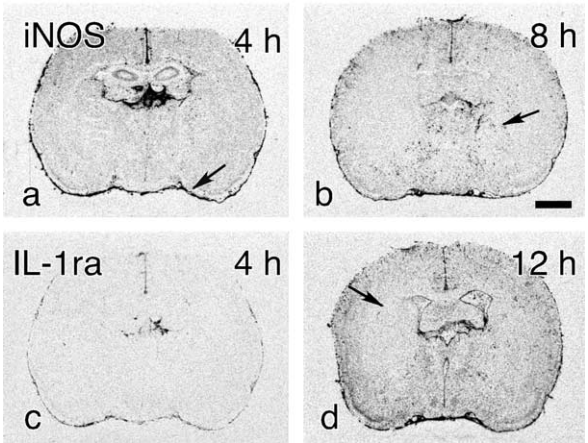

Fig. 8. Film images show iNOS mRNA induction at 4 (a) and 8 h (b) and IL-1ra mRNA induction at 4 (c) and 12 h (d) following i.c.v. IL-1β administration. Scale bar = 2 mm.

IL-1ra mRNA. IL-1ra was a late-appearing induced transcript. Induction first appeared lightly in the meninges at 4 h (Fig. 8c), and grew to maximal levels of expression at 12 h (Fig. 8d). Remnants of meningeal labeling were still present at 24 h, corresponding with the locations of the leukocytes.

GFAP mRNA and protein. GFAP mRNA marking of activated astrocytes showed induction above control levels initially along the cannula tract at 0.5 h. At 2 h, the ipsilateral corpus callosum and internal capsule/cerebral peduncle were slightly elevated (Fig. 9a, b). The overall density of labeling increased at 4–12 h (Fig. 9c–f). The characteristic expression-sparse area of the contralateral striatum and cortex could be discerned (Fig. 9e). At 24 h, the overall GFAP mRNA labeling intensity was the densest yet (Fig. 9g, h).

GFAP immunoreactivity showed changes in parallel with the GFAP mRNA induction patterns. A time-dependent increase in the overall staining intensity was seen; at later time points, the individual cells showed hypertrophied processes in all locations examined (Fig. 9j, k).

Iba1 mRNA and protein. The microglial marker iba1 showed a low level of constitutive mRNA expression distributed homogeneously throughout the brain. Induced expression levels first became clear at 4 h in the meninges (Fig. 10a) and near the cannula track. Further increases in iba1 mRNA levels throughout the brain were evident at 8 h (Fig. 10b), and the maximum intensity was seen at 24 h (Fig. 10c). Details of the pattern of iba1 mRNA-positive cells are shown in the substantia nigra and adjacent structures in Fig. 10d–f.

Similarly, immunostaining with the Iba1 antibody showed a constitutive distribution of small cells throughout the brain (data not shown). In a time-dependent fashion, both staining intensity and number of stained cells increased throughout the brain parenchyma and

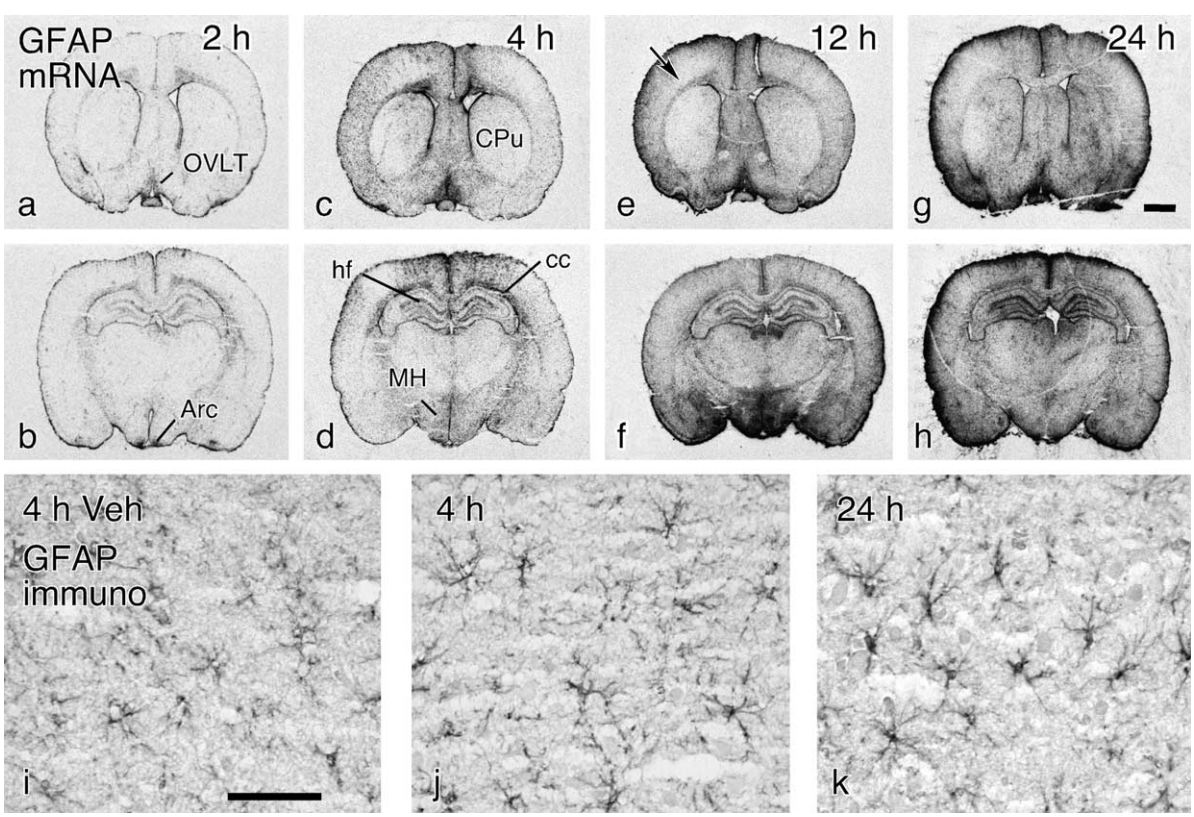

Fig. 9. Film images in a–h show GFAP mRNA expression and induction at 2, 4, 12, and 24 h following i.c.v. IL-1β administration. Arrow in e shows where labeling remains low. Photomicrographs in i–k show GFAP-immunostained astrocytes in the amygdala/cortical area. A vehicle-injected animal is shown in i. In i.c.v. IL-1β-injected animals, the intensity of staining was discernibly increased at 4 h (j) and more dramatically increased at 24 h (k). Scale bars = 2 mm (a–h) and 50 μm (i–k).

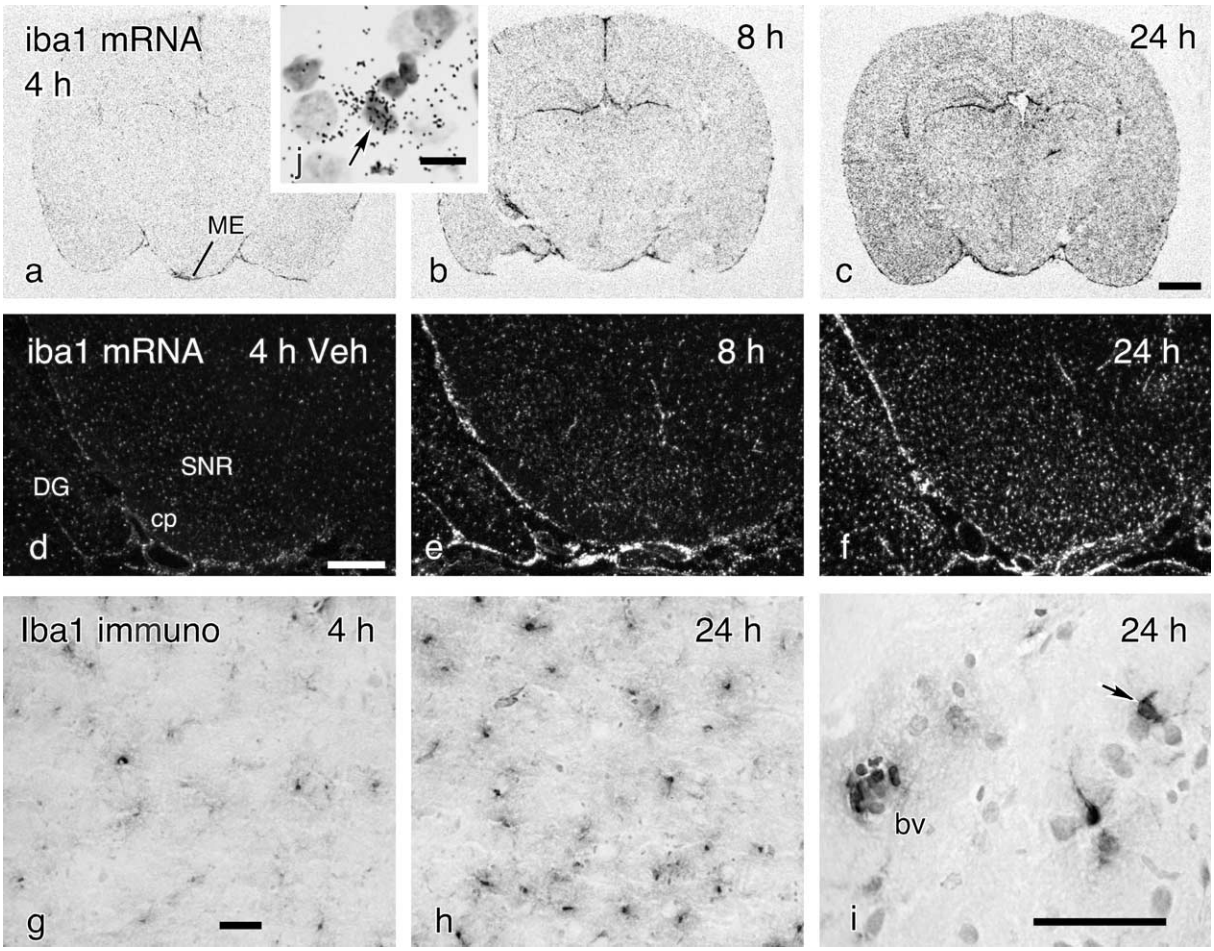

Fig. 10. Film images in a–c show iba1 mRNA induction at 4, 8, and 24 h following i.c.v. IL-1β administration. Dark-field photomicrographs of emulsion-coated slides show iba1 mRNA hybridization in the substantia nigra and adjacent territory in vehicle-injected and IL-1β-injected animals (8 and 24 h) in d–f, respectively. Note that iba1 mRNA expression occurs evenly across the neuropil and also in blood vessels (lines of labeling) and the meninges along the side and base of the mesencephalon at the later time points. Panels g–i show Iba1-immunostained cells in the substantia nigra in IL-1β-injected animals. Stained cells were slightly increased in number over vehicle control at 4 h (g) and much more so at 24 h (h), at which time they could be distinguished as either leukocytes in blood vessels or microglia with processes (arrow in i). The inset (j) shows iba1 mRNA-labeled small cells (arrow) in the thalamus with a Nissl counterstain at high magnification. Scale bars = 2 mm (a–c), 500 μm (d–f), 50 μm (g–i) and 10 μm (insert j).

meninges (Fig. 10g–i). Stained cells at 12 and 24 h were either localized to blood vessels and meninges and were small and devoid of processes, or they were scattered throughout the parenchyma, somewhat larger in size, and had processes (Fig. 10i). The former cells were monocyte/macrophages and the latter were microglia.

Microscopic analysis of probe labeling after i.c.v. IL-1β

Emulsion-dipped, Nissl-stained sections were examined microscopically to aid in the determination of the phenotypes of the various mRNA expressing cells. The vast majority of immune signal mRNAs induced by i.c.v. IL-1β were associated with vascular, meningeal, choroidal, and ventricular ependymal cells of the brain and with the infiltrating leukocytes when they appeared.

IκBα mRNA-positive cells at 0.5 h and 2 h were mostly vascular (Fig. 11a). In the Nissl-counterstained sections that had gone through the hybridization process, the small vascular cells stained darkly and were not further categorized as endothelial, muscular, or perivascular (pericytes or perivascular cells). The majority, however, were endothelial. Throughout the brain, the IκBα mRNA-labeled cells were the smallest and most darkly staining. In addition, choroidal epithelial and ventricular ependymal cells were labeled. At 4 h, IκBα mRNA labeling was diminished in the large external and penetrating vessels but continued to be present in numerous small, dark cells throughout the brain compartment. A greater variety of cell types began to express mRNA, suggesting glial IκBα expression. At 12 h, the labeling was greatly diminished everywhere, leaving leukocytes in the meninges and cisternae labeled (Fig. 12b).

The scattered IL-1β mRNA-positive cells at 0.5–4 h in the meninges and brain appeared to be both meningeal and vascular (endothelial) (Fig. 11b). In addition, some cells of the ventricular ependyma were labeled. The stronger pattern of labeling occurring at 8 h was associated with the vasculature and the infiltrating leukocytes (Fig. 11e), though it was difficult to distinguish between

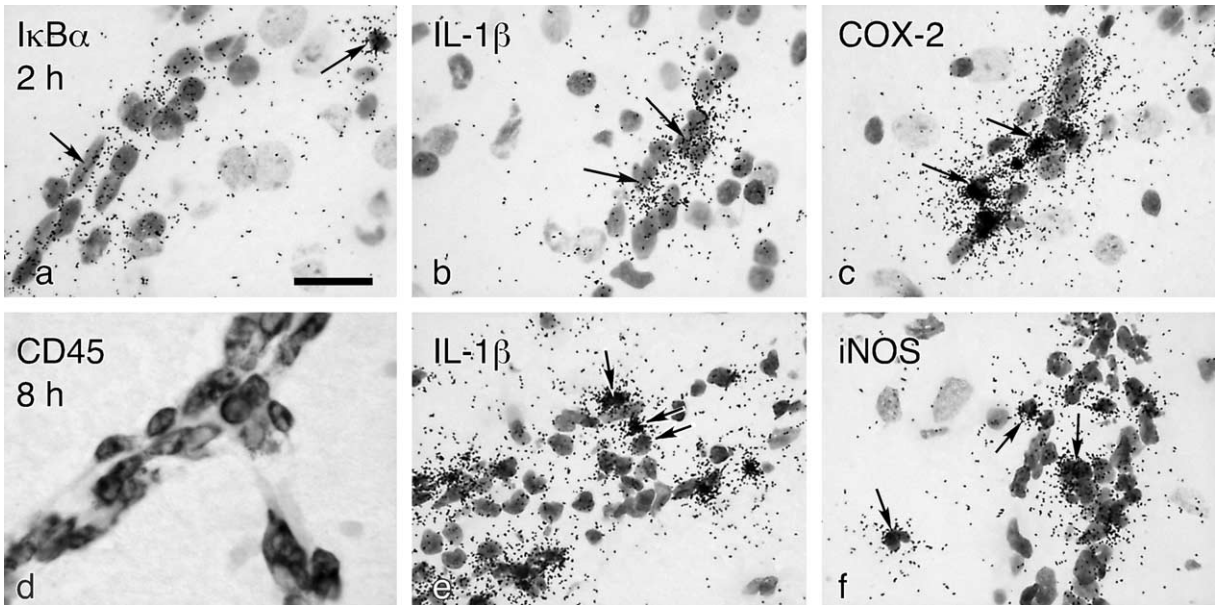

Fig. 11. High-magnification photomicrographs show mRNA-positive cell types in blood vessels prior to (a–c) and after leukocyte adherence to blood vessels (d–f). Photographs are all taken from thalamus. At 2 h after i.c.v. IL-1β injection, IκBα (a), IL-1β (b) and COX-2 (c) mRNAs are induced primarily in the small, dark cells associated with the vessel walls. At 8 h after injection, many of the blood vessels are filled with leukocytes (d), and at these times the vessel wall cells and leukocytes both appear to express IL-1β (e) and iNOS (f) mRNAs. Scale bar = 20 μm.

endothelia and leukocytes in a blood vessel. Labeled cells in the parenchyma were small and conformed in size with the parenchymal leukocytes (Fig. 7f). The pattern correlation with that of leukocytes was quite strong overall. In CD45-positive cell clusters in the meninges, select cells were IL-1β mRNA-positive (Fig. 12c).

IL-1R1 mRNA labeling was observed clearly in the endothelia, arachnoid, choroid plexus, and ventricular ependyma. When leukocytes appeared in the meninges and blood vessels, they also expressed the receptor mRNA (Fig. 12d).

Induced COX-2 mRNA was mainly associated with vascular endothelia (Fig. 11c). Expression disappeared as the leukocyte invasion became strong. However, some of the leukocytes expressed COX-2 mRNA (Fig. 12g), especially early in the time course. In contrast, IL-1ra (Fig. 12e) and iNOS mRNA expressing cells (Fig. 12f) were closely associated temporally and spatially

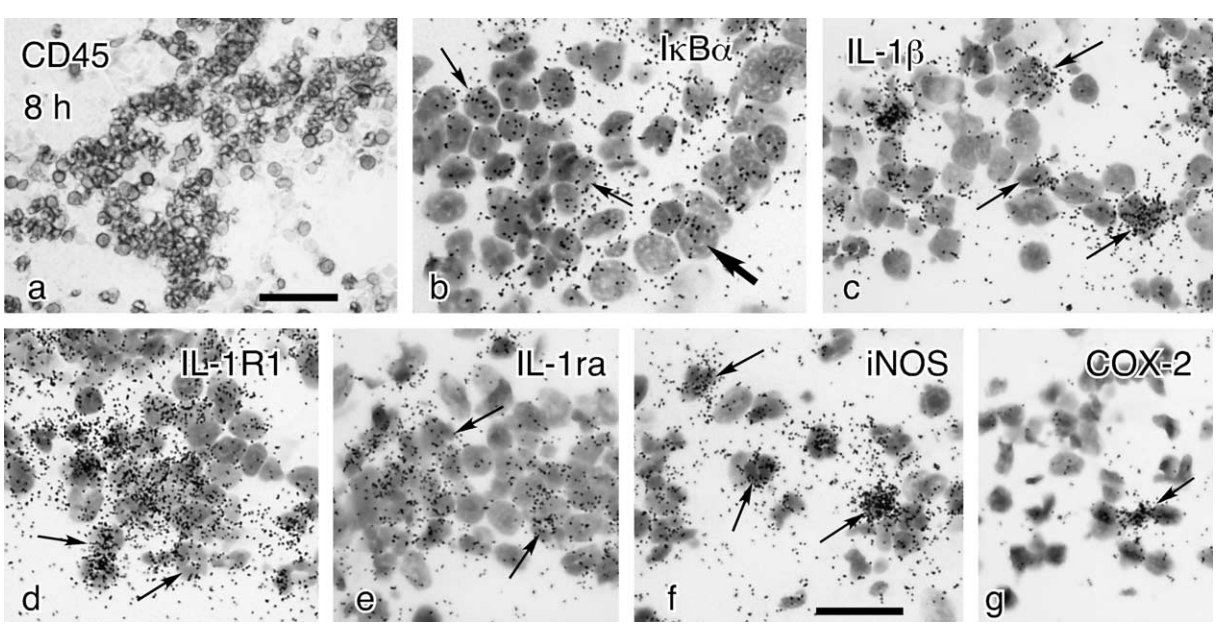

Fig. 12. Bright-field photomicrographs of an identified clump of infiltrating leukocytes located against the velum interpositum just above the habenula. The cells are CD45-positive (a), and subsets of these leukocytes express IκBα (b), IL-1β (c), IL-1R1 (d), IL-1ra (e), iNOS (f), and COX-2 (g) mRNAs. Arrows point to examples of labeled cells. Thick arrow in b points to the epithelial cells of the velum, which is also labeled. Scale bars = 50 μm (a) and 20 μm (b–g).

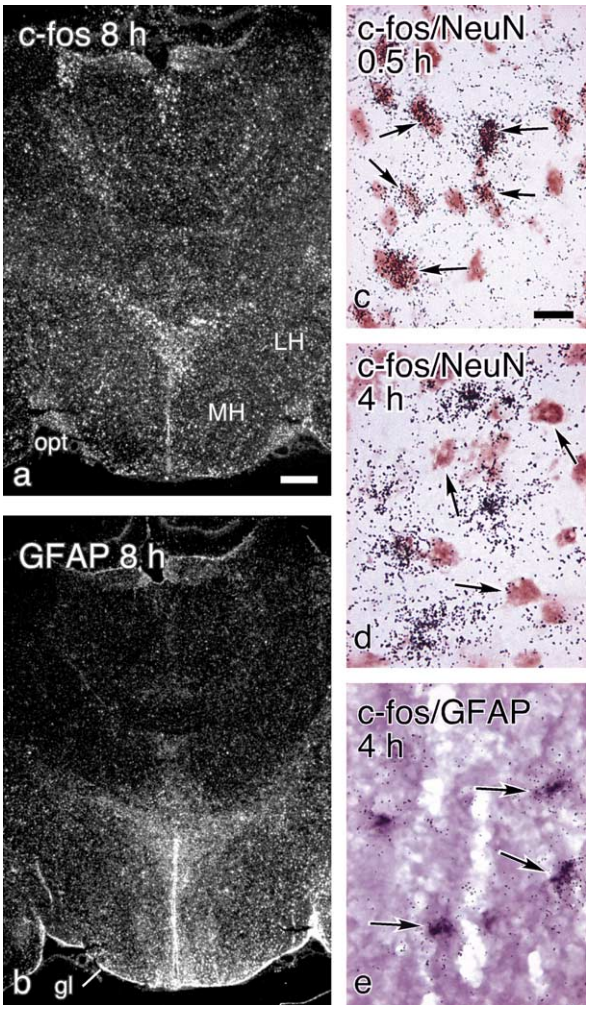

Fig. 13. Low-magnification dark-field photomicrographs of emulsion-coated sections at the level of the PVN show the relationship of c-fos (a) and GFAP (b) mRNAs induced by i.c.v. IL-1β at 8 h. Double-label marking of c-fos mRNA and NeuN immunohistochemistry at 0.5 h (c) and 4 h (d) in the thalamus shows the switch from neuronal (co-localization) to non-neuronal labeling (non co-localization). Arrows point to examples of c-fos mRNA-positive neurons in c and c-fos mRNA-negative neurons in d. Double label of c-fos (^{35}S-labeled) mRNA with GFAP (digoxigenin-labeled) mRNA at 4 h shows co-localization (e) of silver grains and blue–black digoxigenin (arrows). Scale bars = 0.5 mm (a, b) and 20 μm (c–e).

with the CD45-positive cells. Expression of iNOS mRNA in small vascular-associated cells in the thalamus is shown in Fig. 11f.

In contrast with the vascular labeling seen for the inflammatory markers, the cells expressing c-fos, GFAP, and iba1 mRNAs were typically larger and less darkly Nissl-stained (e.g. Fig. 10j). They were also more evenly distributed throughout the neuropil and less likely to be associated with blood vessels. Figure 13 shows the similar patterns of c-fos and GFAP mRNA induction at the level of the PVN. Double-label analysis confirmed that the majority of c-fos mRNA-positive cells early after i.c.v. IL-1β injection were neurons (Fig. 13c), but later they were typically non-neuronal (Fig. 13d) and instead tended to be astrocytes (Fig. 13e).

Response to i.v. IL-1β administration

A battery of markers was applied to brain sections from rats given i.v. IL-1β. The c-fos, IκBα, MCP-1, GFAP, iba1, COX-2, and IL-1β ribonucleotide probes and the CD45, ICAM-1, GFAP, and Iba1 antibodies were applied to the tissue. Of the examined genes, only IκBα, COX-2, and MCP-1 mRNAs were induced (Fig. 14a–i). The induction patterns of IκBα and COX-2 were widespread and uniform throughout the vasculature at 2 h (Fig. 14b, e), and the signal levels returned to baseline at 12 h (Fig. 14c, f). Quantification of the IκBα mRNA signal strength was performed and compared with that after i.c.v. IL-1β administration. At the PVN level quantified, i.v. vehicle-injected animals at 2 and 12 h showed densities of 80–120 d.p.m./mg in structures ranging from the caudate–putamen (lowest density) to basal meninges (highest density). These density measurements include background hybridization levels. At 2 h after i.v. IL-1β administration, densities were bilaterally and evenly increased in the parenchyma – to approximately 200 d.p.m./mg in the caudate–putamen, thalamus, hypothalamus, white matter, and neocortex – and more strongly increased to 400 d.p.m./mg in the meninges. Levels returned to baseline by 12 h. In comparison, after i.c.v. IL-1β administration, IκBα mRNA levels were elevated at 0.5, 2, and 4 h by similar amounts in the parenchymal structures – i.e. to approximately 200 d.p.m./mg in the caudate–putamen, thalamus, hypothalamus, white matter, and cortex – whereas the meninges were elevated to approximately 1000 d.p.m./mg. Measurements of radioactivity levels of COX-2 mRNA showed parallel findings; at the 2-h time point, similar increases over background levels of expression were seen in the parenchyma after both i.v. and i.c.v. IL-1β administrations, whereas in the meninges, the increase was much greater after i.c.v. injections.

Induction of MCP-1 mRNA after i.v. IL-1β was relatively confined to the choroid plexus, SFO, and scattered blood vessels at 2 h (Fig. 14g), and labeling was absent at 12 h. c-fos mRNA showed induction at 2 h in restricted locations such as the circumventricular organs, nucleus of the solitary tract, and PVN. The labeling returned to baseline at 12 h (data not shown).

The other mRNAs showed no induction at either time point (i.v. vehicle- and IL-1β-injected animals are compared at the 12-h time point in Fig. 14j–o). In agreement with the negative data from the hybridization experiments, immunohistochemistry showed no change in the appearance, number, or staining intensity of ICAM-1 in blood vessels (Fig. 15a, b), CD45 in scattered cells in the meninges (Fig. 15c, d), or GFAP and Iba1 in astrocytes and microglia throughout the brain parenchyma (Fig. 15e–h).

Summary of temporal pattern

Figure 16 shows a summary of the timing and location of mRNA induction and immunostaining changes mapped in this study. Links are drawn between the

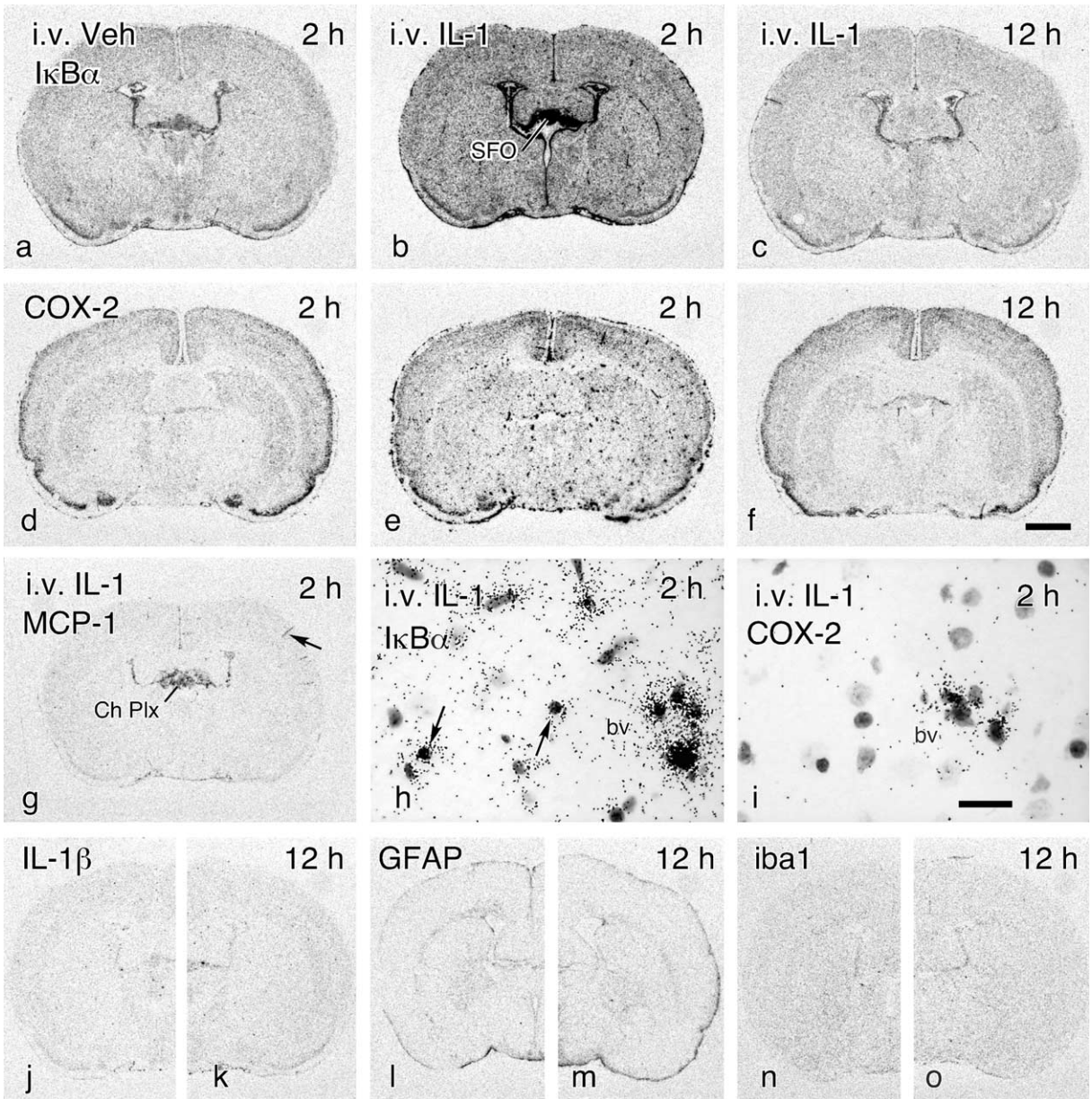

Fig. 14. Film images show mRNA expression of IκBα (a–c), COX-2 (d–f), and MCP-1 (g) mRNAs in the SFO and vasculature after i.v. injection of vehicle (a, d) or IL-1β at 2 h (b, e, g) or 12 h (c, f) after i.v. injection. Arrow in g points to a labeled cortical blood vessel. The expression levels return to baseline (Vehicle levels) at 12 h, as shown. High-magnification photomicrographs of labeling show induced expression of IκBα (h) and COX-2 (i) mRNAs at 2 h following i.v. IL-1β. Unresponsive genes, shown in pairs (vehicle on left and i.v. IL-1β-treated on right) in film images, are IL-1β (j, k), GFAP (l, m), and iba1 (n, o). Scale bars = 2 mm (a–g and j–o) and 20 μm (h–i).

events to suggest the causal basis of the sequential activation.

DISCUSSION

The present results demonstrate that 100 ng of recombinant rat IL-1β infused into the lateral ventricle of awake rats (1) rapidly induced widespread vascular expression of mRNAs for several key immune signaling genes, (2) up-regulated vascular ICAM-1 immunostaining, (3) caused widespread leukocyte infiltration, and (4) triggered a long lasting activation of astrocytes and microglia throughout the entire brain. This dramatic and widespread response has not been seen following i.c.v. injection of other bioactive molecules, so a unique role for IL-1β in brain immune signaling is suggested (Fig. 16). The response was also not seen after i.v. administration of IL-1β in spite of the fact that both routes of administration result in vascular induction of IκBα and COX-2 mRNAs (this study) and fever as reported in other studies using a range of doses and IL-1β preparations (Dascombe et al., 1989).

A number of additional novel findings emerged. (1) The pattern of widespread IκBα and COX-2 mRNA induction on blood vessels argues that IL-1β flows in

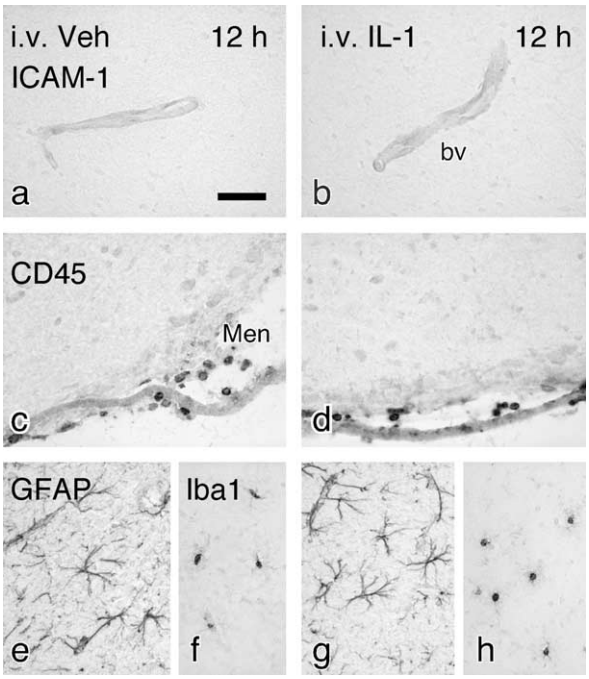

Fig. 15. Bright-field photomicrographs show immunostaining of selected sections in i.v. vehicle (left side) or i.v. IL-1β (right side) animals killed 12 h after administration. None of the illustrated markers was affected by i.v. IL-1β, as shown. Markers are ICAM-1 (a, b), CD45 (c, d), GFAP (e, g), and Iba1 (f, h). Scale bar = 50 μm.

perivascular channels to reach target receptors on endothelia. (2) The i.c.v. IL-1β effects are very different from i.c.v. TNF-α effects with regard to spatial distribution, phenotype, and mRNA expression profile of responsive cells. (3) Induction of mRNA for the chemokine MCP-1 is largely confined to blood vessels and is not found in glia or other parenchymal cells. (4) Leukocytes enter the brain parenchyma beginning at around 8 h and are still present at 24 h. (5) Infiltrating leukocytes express cytokine (IL-1β and IL-1ra), cytokine receptor (IL-1R1), and iNOS mRNAs. (6) The widespread activation of microglia and astrocytes includes induction of c-fos mRNA in astrocytes. (7) Parenchymal cytokine mRNA expression comes from leukocytes and not from astrocytes or microglia (contrasting with i.v. LPS, chronic brain inflammation/injury models, and i.c.v. TNF-α and high-dose i.c.v. IL-1β). (8) Differential cytokine induction profiles in stromal cells versus leukocytes indicate response selectivity in the immune molecule signaling system.

The early induction pattern: ventricular, cisternal, and perivascular flow

Following i.c.v. injection of radiolabeled inulin or sucrose in awake rats, the tracer molecules follow CSF flow in the ventricles and subarachnoid spaces of the major cisternae, enter perivascular spaces, and diffuse slowly into the brain parenchyma with a gradient of decreasing density (Ghersi-Egea et al., 1996; Proescholdt et al., 2000). A similar distribution pattern for i.c.v. IL-1β can be visualized by immunohistochemistry (Konsman et al., 2000). In the present study, evidence of this pattern can be discerned at the earliest time points after i.c.v. IL-1β injection.

However, periventricular and intraparenchymal gradients of gene induction were almost completely overshadowed by the widespread IκBα and COX-2 mRNA induction throughout the vasculature. Of course, the vasculature is where most IL-1β receptors (IL-1R1) are expressed (Ericsson et al., 1995), and they are expressed on both the brain side (abluminal) as well as the blood side (luminal) of the endothelial cells (Cao et al., 2001). Still, the result was quite surprising given the inaccessibility of these locations to IL-1β circulating in the CSF. I.c.v. IL-1β could gain access to these distant sites (1) by leaving the brain and entering the blood or (2) by traveling in perivascular channels. Although i.c.v. IL-1β is cleared from the brain compartment into the peripheral blood (Chen and Reichlin, 1999), the peripheral route of access to the vasculature seems unlikely because of the very different outcomes observed when IL-1β was injected directly into the blood, resulting in a more homogeneous IκBα mRNA induction pattern and absence of sequelae (see below). However, it is also possible that a bolus of i.v. IL-1β does not simulate the kinetics of IL-1β leaked into the blood from the brain, and/or that IL-1β in either compartment induces the production of other unidentified bioactive substances that affect the response. Nevertheless, travel of IL-1β in perivascular channels seems to be a more likely mechanism of vascular activation.

Perivascular transport is not easily documented with radiolabeled tracers like [^{14}C]inulin (Proescholdt et al., 2000), but it has been dramatically shown using horseradish peroxidase (Rennels et al., 1985; Stoodley et al., 1996). The sensitive, non-quantitative reaction with tetramethylbenzidine allows clear visualization of the 'paravascular' flow pathways (Rennels et al., 1985). Interestingly, molecules are propelled along these routes by arterial pulsations (Rennels et al., 1985), so it is possible that the experimental outcome is dependent on the arousal level of the animal.

The late induction pattern mirrors the early pattern – role of the vasculature

The pattern of MCP-1 mRNA expression and ICAM-1 immunostaining in blood vessels and the location of subsequent CD45-stained leukocyte infiltration mirrored the initial pattern of IκBα mRNA labeling. Areas that are known to be preferentially suffused with [^{14}C]inulin, like the cortex along the longitudinal fissure and the hippocampal fissure (Proescholdt et al., 2000), show greater leukocyte influx. Areas that receive very little [^{14}C]inulin following a unilateral injection into the lateral ventricle, namely the contralateral striatum and overlying deep cortical layers, were notably unresponsive in both the initial and late phases. Thus, it can be speculated that the early perivascular diffusion of IL-1β and its actions on the endothelia initiated and directed the peripheral immune response. However, this conclusion needs to be confirmed by additional studies.

Chemokine induction and cell adhesion molecule

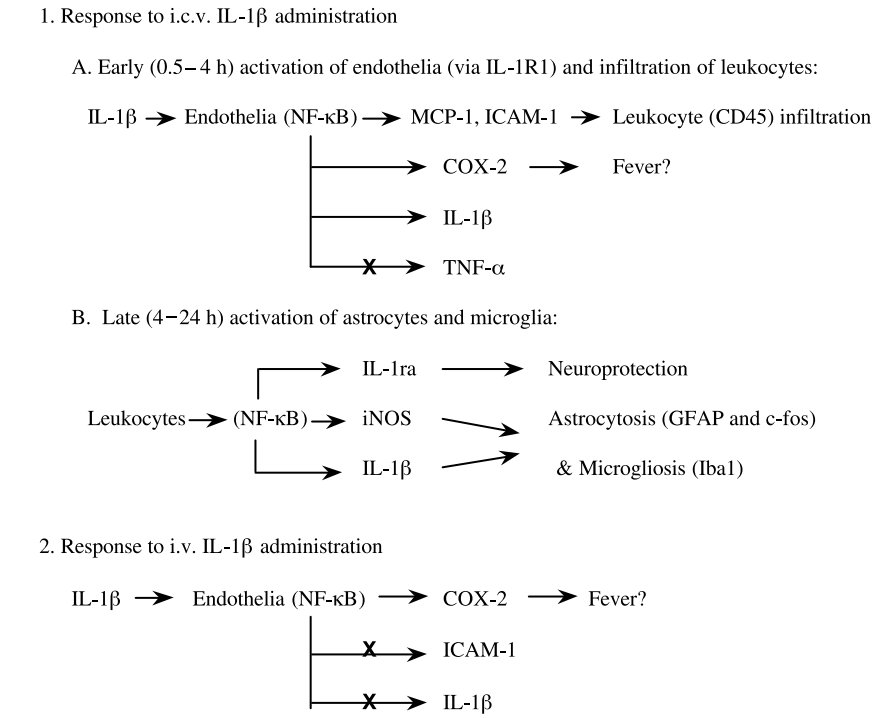

Fig. 16. Summary of the timing of mRNA induction with possible links drawn between the mRNAs suggests the causal nature of the sequential activation. The early appearance of IκBα mRNA expression in the endothelia indicates that the NF-κB transcription factor mechanism was active in these cells (as reviewed elsewhere (Quan et al., 1997; Laflamme et al., 1999)). However, only some of its target genes were transcribed. Importantly, MCP-1 and ICAM-1 (and perhaps other chemokines and cell adhesion molecules) were up-regulated on the endothelia, and this attracted leukocyte migration into the brain. The leukocytes selectively expressed IL-1β and iNOS but not TNF-α mRNAs. That recruited leukocytes produce IL-1β but not TNF-α in the CSF has been determined in an experimental meningitis study (Ostergaard et al., 2000). The pro-inflammatory (IL-1β and iNOS) molecules expressed by the leukocytes may have caused the widespread activation of astrocytes (GFAP) and microglia (Iba1) that was observed. Delayed expression of anti-inflammatory molecules (IL-1ra) may be protective in a general way and may help to terminate the inflammatory processes. In contrast, after i.v. IL-1β administration, IκBα and COX-2 mRNAs were induced in endothelia or perivascular cells, but the other sequelae were absent.

expression on blood vessels is a key mediator of leukocyte emigration into the CSF and brain. Their role has been noted in meningitis, a disease characterized by marked CSF extravasation of leukocytes (Fassbender et al., 1997; Lahrtz et al., 1998). Two representative molecules were mapped in this study to clarify their spatio-temporal relationship to i.c.v. IL-1β-induced leukocyte entry. The gene for MCP-1, a powerful monocyte attractant, is induced in endothelia by IL-1β *in vitro* (Rollins et al., 1990) and *in vivo* (Thibeault et al., 2001). Its receptor, CCR2, is expressed on leukocytes (Charo et al., 1994) and is co-localized with ED1-positive monocytes/activated microglia following excitotoxic brain injury (Galasso et al., 2000). Similarly, ICAM-1 is induced on endothelia by IL-1β and plays an important role in leukocyte diapedesis (Greenwood et al., 1995). ICAM-1 (CD54) is a ligand for integrins (CD11a, CD11b, CD18) and CD43 expressed on leukocytes (reviewed in (Lee and Benveniste, 1999). Other molecules worthy of study would be chemokines in the CXC family that attract neutrophils and adhesion molecules like VCAM-1 that attract leukocytes.

Leukocyte entry as meningitis

As shown in this and other studies, i.c.v. IL-1β administration produces a condition that mimics bacterial and viral meningitis (Ramilo et al., 1990; Quagliarello et al., 1991; Tang et al., 1996). In the meningitis studies, parenchymal entry of leukocytes is not described, so the localized nature of the neuropathology is not explained. In patients and experimental animals with bacterial meningitis, leukocyte-mediated selective cell loss in the medial parts of the dentate gyrus is a predominant feature (Braun et al., 1999). This is a location where preferential homing of leukocytes was observed (Fig. 7). Several mRNAs were strongly expressed by the leukocytes, notably iNOS and IL-1β. The transient production of nitric oxide, suggested by the iNOS mRNA expression, may initiate an injury response, as has been suggested in neurodegeneration (Dawson and Dawson, 1996; Nakanishi et al., 2001) and meningitis models (Braun et al., 1999). Nitric oxide also contributes in complex ways to leukocyte behavior and adhesion (MacMicking et al., 1997).

Activation of astrocytes and microglia

The observed Iba1 and GFAP changes are consistent with microglial activation (Graeber et al., 1998) and reactive astrocytosis (Giulian and Lachman, 1985; Eddleston and Mucke, 1993), respectively. Induction of c-fos message and protein in astrocytes has been

associated with their proliferation and differentiation (Dragunow et al., 1990; Hisanaga et al., 1990). Interestingly, neither glial type appeared to significantly express cytokines (IL-1β, TNF-α, IL-1ra), based on location and morphology of the mRNA-positive cells. Microglial expression of IL-1β immunoreactivity has been induced by i.c.v. IL-1β, but only after very high doses (5 μg) were administered (Konsman et al., 2000). Similarly, parenchymal microglial cells express IL-1β mRNA following septic but not subseptic doses of LPS injected peripherally (Buttini and Boddeke, 1995; Quan et al., 1999b). Apparent microglial expression of IL-1β mRNA was seen near the cannula tip in this study. Astroglia have been reported to express MCP-1 after brain injury (Glabinski et al., 1996) or viral infection (Conant et al., 1998), but they did not measurably after IL-1β administration in this study.

Stimulus specificity: differential actions of i.c.v. IL-1β versus TNF-α

The effects of i.c.v. IL-1β administration are dramatically different from those of i.c.v. TNF-α administration. IκBα mRNA, as a measure of NF-κB transcriptional activity in cells, is responsive to both pro-inflammatory cytokines (Pahl, 1999), but IL-1β induced the expression of IκBα and COX-2 mRNAs in a widespread vascular response pattern, whereas TNF-α induced IκBα (Nadeau and Rivest, 2000) and COX-2 (Cao et al., 1998) mRNAs in restricted periventricular locations. The most likely explanation for these differences lies in the locations of the respective receptors for the two cytokines. IL-1β receptors (IL-1R1) are located predominantly on vascular endothelia and are constitutively expressed there, whereas TNF-α receptors (p55 and p75) are weakly expressed before TNF-α administration and are subsequently induced by high circulating concentrations of TNF-α (Nadeau and Rivest, 1999).

Consequently, i.c.v. TNF-α induced TNF-α and CD14 mRNA expression in parenchymal microglia (Nadeau and Rivest, 2000), whereas i.c.v. IL-1β did not. Conversely, whereas i.c.v. or intraparenchymal IL-1β effectively induced leukocyte pleocytosis, TNF-α did not (Quagliarello et al., 1991; Anthony et al., 1997; Holmin and Mathiesen, 2000). The combined data suggest complementary roles for the cytokines as paracrine messengers – IL-1β recruits leukocytes whereas TNF-α stimulates cytokine production by microglia.

Stimulus specificity: i.c.v. versus i.v. IL-1β

A dramatic finding in this study is that both i.c.v. and i.v. IL-1β induced IκBα and COX-2 mRNA expression in blood vessels, but only i.c.v. IL-1β elicited the subsequent cascade of events reported herein. It is possible that components of the signal cascade located on the luminal side of the endothelial cell are down-regulated because that side is normally exposed to a wide variety of immunogenic stimuli. It is also possible that the effective dose of IL-1β was different in the two administration paradigms, even though the IκBα and COX-2 mRNA vascular response magnitudes were similar throughout the parenchymal vasculature at the time points measured. The meningeal mRNA expression levels were elevated more after i.c.v. than i.v. IL-1β administration at 2 h, reflecting preferential meningeal access of i.c.v. IL-1β flowing in the CSF. This outcome might help to explain the leukocyte extravasation at the meninges after i.c.v. IL-1β, but it does not explain the *trans*-vascular extravasation that was observed throughout the parenchyma.

IL-1β has been shown *in vitro* to increase adhesiveness of leukocytes to endothelium via adhesion molecules such as ICAM-1 (Bevilacqua et al., 1989). Interestingly, when an endothelial monolayer is stimulated with IL-1β from the abluminal surface, there is a strongly preferential up-regulation of ICAM-1 on the luminal surface (Staykova et al., 2000). IL-1β is not only a more potent stimulator of ICAM-1 when presented on the abluminal (brain) side of the blood vessel, but it also preferentially stimulates ICAM-1 induction on the luminal (blood) side. This directional sensitivity might in part explain the more potent and differential actions of i.c.v. contrasted with i.v. IL-1β.

Response specificity

The transcription of IκBα mRNA results from DNA-binding of NF-κB (Miyamoto and Verma, 1995) and, therefore, should indicate that this transcriptional pathway has been activated (Quan et al., 1997). NF-κB can initiate the transcription of over 150 target genes, including all of the genes examined in this study (Pahl, 1999). It is therefore surprising that the induction of IκBα mRNA in the endothelia was associated closely with the induction of COX-2 and MCP-1 mRNAs and to a lesser extent IL-1β, but not with TNF-α, IL-1ra, or iNOS mRNAs, whereas IκBα mRNA induction in the leukocytes was associated with the selective induction of IL-1β, IL-1ra, and iNOS mRNAs but not at all or minimally with TNF-α, COX-2, and MCP-1 mRNAs in these cells. The differences illustrate that additional transcription factors may be required to fully activate the transcriptional machinery for a given gene. These factors are likely to be different for different cells and different circumstances. There may be thresholds for transcriptional activation as well, and clearly there are unique, characteristic transcriptional time courses. The selective responses highlight the importance of *in vivo* experiments.

SUMMARY

A new mechanism for signaling between the brain and the periphery is proposed. IL-1β in the CSF reaches its target receptors on the abluminal side of vascular endothelia via perivascular flow routes, up-regulates chemokines and cell adhesion molecules in those locations, and rapidly initiates site-specific leukocyte (myeloid lineage) trafficking into the brain. The leukocytes produce IL-1β and nitric oxide, and astrocytes and microglia become

activated. It is proposed that this is a unique action of i.c.v. IL-1β that is not shared by TNF-α. Additionally, i.c.v. IL-1β appears to be a much more potent stimulus than i.v. IL-1β to induce vascular responses that subsequently recruit peripheral immune cells into the brain. Because we show that IL-1β in the CSF orchestrates a cascade of molecular events that lead to leukocyte extravasation, we demonstrate a mechanism by which immune privilege can be dynamically modified.

Acknowledgements—This work was supported by the NIMH Intramural Research Program and the Fogarty International Center.

REFERENCES

Anforth, H.R., Bluthe, R.M., Bristow, A., Hopkins, S., Lenczowski, M.J., Luheshi, G., Lundkvist, J., Michaud, B., Mistry, Y., Van Dam, A.-M., Zhen, C., Dantzer, R., Poole, S., Rothwell, N.J., Tilders, F.J., Wollman, E.E., 1998. Biological activity and brain actions of recombinant rat interleukin-1alpha and interleukin-1beta. Eur. Cytokine Netw. 9, 279–288.

Anthony, D.C., Bolton, S.J., Fearn, S., Perry, V.H., 1997. Age-related effects of interleukin-1β on polymorphonuclear neutrophil-dependent increases in blood–brain barrier permeability in rats. Brain 120, 435–444.

Bevilacqua, M.P., Stengelin, S., Gimbrone, M.A., Seed, B., 1989. Endothelial leukocyte adhesion molecule 1: an inducible receptor for neutrophils related to complement regulatory proteins and lectins. Science 243, 1160–1165.

Braun, J.S., Novak, R., Herzog, K.-H., Bodner, S.M., Cleveland, J.L., Tuomanen, E.I., 1999. Neuroprotection by a caspase inhibitor in acute bacterial meningitis. Nat. Med. 5, 298–302.

Buttini, M., Boddeke, H., 1995. Peripheral lipopolysaccharide stimulation induces interleukin-1β messenger RNA in rat brain microglial cells. Neuroscience 65, 523–530.

Cao, C., Matsumura, K., Ozaki, M., Watanabe, Y., 1999. Lipopolysaccharide injected into the cerebral ventricle evokes fever through induction of cyclooxygenase-2 in brain endothelial cells. J. Neurosci. 19, 716–725.

Cao, C., Matsumura, K., Shirakawa, N., Maeda, M., Jikihara, I., Kobayashi, S., Watanabe, Y., 2001. Pyrogenic cytokines injected into the rat cerebral ventricle induce cyclooxygenase-2 in brain endothelial cells and also upregulate their receptors. Eur. J. Neurosci. 13, 1781–1790.

Cao, C., Matsumura, K., Yamagata, K., Watanabe, Y., 1998. Cyclooxygenase-2 is induced in brain blood vessels during fever evoked by peripheral or central administration of tumor necrosis factor. Brain Res. Mol. Brain Res. 56, 45–56.

Charo, I.F., Myers, S.J., Herman, A., Franci, C., Connolly, A.J., Coughlin, S.R., 1994. Molecular cloning and functional expression of two monocyte chemoattractant protein 1 receptors reveals alternative splicing of the carboxyl-terminal tails. Proc. Natl. Acad. Sci. USA 91, 2752–2756.

Chen, G., Reichlin, S., 1999. Mechanisms by which blood levels of interleukin-6 (IL-6) are elevated after intracerebroventricular injection of IL-1β in the rat: neural versus humoral control. Endocrinology 140, 5549–5555.

Conant, K., Garzino-Demo, A., Nath, A., McArthur, J.C., Halliday, W., Power, C., Gallo, R.C., Major, E.O., 1998. Induction of monocyte chemoattractant protein-1 in HIV-1 Tat-stimulated astrocytes and elevation in AIDS dementia. Proc. Natl. Acad. Sci. USA 95, 3117–3121.

Dascombe, M.J., Rothwell, N.J., Sagay, B.O., Stock, M.J., 1989. Pyrogenic and thermogenic effects of interleukin 1 beta in the rat. Am. J. Physiol. 256, E7–E11.

Dawson, V.L., Dawson, T.M., 1996. Nitric oxide neurotoxicity. J. Chem. Neuroanat. 10, 179–190.

Dragunow, M., de Castro, D., Faull, R.L., 1990. Induction of Fos in glia-like cells after focal brain injury but not during wallerian degeneration. Brain Res. 527, 41–54.

Eddleston, M., Mucke, L., 1993. Molecular profile of reactive astrocytes – implications for their role in neurologic disease. Neuroscience 54, 15–36.

Ericsson, A., Liu, C., Hart, R.P., Sawchenko, P.E., 1995. Type 1 interleukin-1 receptor in the rat brain: distribution, regulation, and relationship to sites of IL-1-induced cellular activation. J. Comp. Neurol. 361, 681–698.

Eriksson, C., Nobel, S., Winblad, B., Schultzberg, M., 2000. Expression of interleukin 1α and β, and interleukin 1 receptor antagonist mRNA in the rat central nervous system after peripheral administration of lipopolysaccharides. Cytokine 12, 423–431.

Fassbender, K., Schminke, U., Ries, S., Ragoschke, A., Kischka, U., Fatar, M., Hennerici, M., 1997. Endothelial-derived adhesion molecules in bacterial meningitis: association to cytokine release and intrathecal leukocyte-recruitment. J. Neuroimmunol. 74, 130–134.

Galasso, J.M., Miller, M.J., Cowell, R.M., Harrison, J.K., Warren, J.S., Silverstein, F.S., 2000. Acute excitotoxic injury induces expression of monocyte chemoattractant protein-1 and its receptor, CCR2, in neonatal rat brain. Exp. Neurol. 165, 295–305.

Garabedian, B.V., Lemaigre-Dubreuil, Y., Mariani, J., 2000. Central origin of IL-1β produced during peripheral inflammation: role of meninges. Brain Res. Mol. Brain Res. 75, 259–263.

Ghersi-Egea, J.F., Finnegan, W., Chen, J.L., Fenstermacher, J.D., 1996. Rapid distribution of intraventricularly administered sucrose into cerebrospinal fluid cisterns via subarachnoid velae in rat. Neuroscience 75, 1271–1288.

Giulian, D., Lachman, L.B., 1985. Interleukin-1 stimulation of astroglial proliferation after brain injury. Science 228, 497–499.

Glabinski, A.R., Balasingam, V., Tani, M., Kunkel, S.L., Strieter, R.M., Yong, V.W., Ransohoff, R.M., 1996. Chemokine monocyte chemoattractant protein-1 is expressed by astrocytes after mechanical injury to the brain. J. Immunol. 156, 4363–4368.

Graeber, M.B., Lopez-Redondo, F., Ikoma, E., Ishikawa, M., Imai, Y., Nakajima, K., Kreutzberg, G.W., Kohsaka, S., 1998. The microglia/macrophage response in the neonatal rat facial nucleus following axotomy. Brain Res. 813, 241–253.

Greenwood, J., Wang, Y., Calder, V.L., 1995. Lymphocyte adhesion and transendothelial migration in the central nervous system: the role of LFA-1, ICAM-1, VLA-4 and VCAM-1. Immunology 86, 408–415.

Griffin, D.E., 1997. Cytokines in the brain during viral infection: clues to HIV-associated dementia. J. Clin. Invest. 100, 2948–2951.

Herkenham, M., Lee, H.Y., Baker, R.A., 1998. Temporal and spatial patterns of *c-fos* mRNA induced by intravenous interleukin-1: a cascade of non-neuronal cellular activation at the blood–brain barrier. J. Comp. Neurol. 400, 175–196.

Herx, L.M., Rivest, S., Yong, V.W., 2000. Central nervous system-initiated inflammation and neurotrophism in trauma: IL-1β is required for the production of ciliary neurotrophic factor. J. Immunol. 165, 2232–2239.

Hisanaga, K., Sagar, S.M., Hicks, K.J., Swanson, R.A., Sharp, F.R., 1990. c-fos proto-oncogene expression in astrocytes associated with differentiation or proliferation but not depolarization. Brain Res. Mol. Brain Res. 8, 69–75.

Hohmann, A.G., Herkenham, M., 1999. Localization of central cannabinoid CB1 receptor messenger RNA in neuronal subpopulations of rat dorsal root ganglia: a double-label *in situ* hybridization study. Neuroscience 90, 923–931.

Holmin, S., Mathiesen, T., 2000. Intracerebral administration of interleukin-1β and induction of inflammation, apoptosis, and vasogenic edema. J. Neurosurg. 92, 108–120.

Imai, Y., Ibata, I., Ito, D., Ohsawa, K., Kohsaka, S., 1996. A novel gene iba1 in the major histocompatibility complex class III region encoding an EF hand protein expressed in a monocytic lineage. Biochem. Biophys. Res. Commun. 224, 855–862.
Ito, D., Imai, Y., Ohsawa, K., Nakajima, K., Fukuuchi, Y., Kohsaka, S., 1998. Microglia-specific localisation of a novel calcium binding protein, Iba1. Brain Res. Mol. Brain Res. 57, 1–9.
Konsman, J.P., Kelley, K., Dantzer, R., 1999. Temporal and spatial relationships between lipopolysaccharide-induced expression of Fos, interleukin-1β and inducible nitric oxide synthase in rat brain. Neuroscience 89, 535–548.
Konsman, J.P., Tridon, V., Dantzer, R., 2000. Diffusion and action of intracerebroventricularly injected interleukin-1 in the CNS. Neuroscience 101, 957–967.
Laflamme, N., Lacroix, S., Rivest, S., 1999. An essential role of interleukin-1β in mediating NF-κB activity and COX-2 transcription in cells of the blood–brain barrier in response to a systemic and localized inflammation but not during endotoxemia. J. Neurosci. 19, 10923–10930.
Lahrtz, F., Piali, L., Spanaus, K.S., Seebach, J., Fontana, A., 1998. Chemokines and chemotaxis of leukocytes in infectious meningitis. J. Neuroimmunol. 85, 33–43.
Lee, S.J., Benveniste, E.N., 1999. Adhesion molecule expression and regulation on cells of the central nervous system. J. Neuroimmunol. 98, 77–88.
MacMicking, J., Xie, Q.W., Nathan, C., 1997. Nitric oxide and macrophage function. Annu. Rev. Immunol. 15, 323–350.
Miyamoto, S., Verma, I.M., 1995. Rel/NF-κB/IκB story. Adv. Cancer Res. 66, 255–292.
Mrak, R.E., Griffin, W.S., 2000. Interleukin-1 and the immunogenetics of Alzheimer disease. J. Neuropathol. Exp. Neurol. 59, 471–476.
Mustafa, M.M., Lebel, M.H., Ramilo, O., Olsen, K.D., Reisch, J.S., Beutler, B., McCracken, G.H., Jr., 1989. Correlation of interleukin-1 beta and cachectin concentrations in cerebrospinal fluid and outcome from bacterial meningitis. J. Pediatr. 115, 208–213.
Nadeau, S., Rivest, S., 1999. Effects of circulating tumor necrosis factor on the neuronal activity and expression of the genes encoding the tumor necrosis factor receptors (p55 and p75) in the rat brain: a view from the blood–brain barrier. Neuroscience 93, 1449–1464.
Nadeau, S., Rivest, S., 2000. Role of microglial-derived tumor necrosis factor in mediating CD14 transcription and nuclear factor κ B activity in the brain during endotoxemia. J. Neurosci. 20, 3456–3468.
Nakanishi, H., Zhang, J., Koike, M., Nishioku, T., Okamoto, Y., Kominami, E., von Figura, K., Peters, C., Yamamoto, K., Saftig, P., Uchiyama, Y., 2001. Involvement of nitric oxide released from microglia-macrophages in pathological changes of cathepsin D-deficient mice. J. Neurosci. 21, 7526–7533.
Ostergaard, C., Yieng-Kow, R.V., Benfield, T., Frimodt-Moller, N., Espersen, F., Lundgren, J.D., 2000. Inhibition of leukocyte entry into the brain by the selectin blocker fucoidin decreases interleukin-1 (IL-1) levels but increases IL-8 levels in cerebrospinal fluid during experimental pneumococcal meningitis in rabbits. Infect. Immun. 68, 3153–3157.
Pahl, H.L., 1999. Activators and target genes of Rel/NF-κB transcription factors. Oncogene 18, 6853–6866.
Plata-Salaman, C.R., Ilyin, S.E., Gayle, D., Romanovitch, A., Carbone, K.M., 1999. Persistent Borna disease virus infection of neonatal rats causes brain regional changes of mRNAs for cytokines, cytokine receptor components and neuropeptides. Brain Res. Bull. 49, 441–451.
Proescholdt, M.G., Hutto, B., Brady, L.S., Herkenham, M., 2000. Studies of cerebrospinal fluid flow and penetration into brain following lateral ventricle and cisterna magna injections of the tracer [^{14}C]inulin in rat. Neuroscience 95, 577–592.
Quagliarello, V.J., Wispelwey, B., Long, W.J., Jr., Scheld, W.M., 1991. Recombinant human interleukin-1 induces meningitis and blood–brain barrier injury in the rat. Characterization and comparison with tumor necrosis factor. J. Clin. Invest. 87, 1360–1366.
Quan, N., Mhlanga, J.D.M., Whiteside, M.B., McCoy, A.N., Kristensson, K., Herkenham, M., 1999a. Chronic over-expression of pro-inflammatory cytokines and histopathology in the brains of rats infected with *Trypanosoma brucei*. J. Comp. Neurol. 414, 114–130.
Quan, N., Stern, E.L., Whiteside, M.B., Herkenham, M., 1999b. Induction of pro-inflammatory cytokine mRNAs in the brain after peripheral injection of subseptic doses of lipopolysaccharide in the rat. J. Neuroimmunol. 93, 72–80.
Quan, N., Sundar, S.K., Weiss, J.M., 1994. Induction of interleukin-1 in various brain regions after peripheral and central injections of lipopolysaccharide. J. Neuroimmunol. 49, 125–134.
Quan, N., Whiteside, M., Herkenham, M., 1998. Time course and localization patterns of interleukin-1β messenger RNA expression in brain and pituitary after peripheral administration of lipopolysaccharide. Neuroscience 83, 281–293.
Quan, N., Whiteside, M., Kim, L., Herkenham, M., 1997. Induction of inhibitory factor κBα mRNA in the central nervous system after peripheral lipopolysaccharide administration: An *in situ* hybridization histochemistry study in the rat. Proc. Natl. Acad. Sci. USA 94, 10985–10990.
Ramilo, O., Saez-Llorens, X., Mertsola, J., Jafari, H., Olsen, K.D., Hansen, E.J., Yoshinaga, M., Ohkawara, S., Nariuchi, H., McCracken, G.H., Jr., 1990. Tumor necrosis factor alpha/cachectin and interleukin 1 beta initiate meningeal inflammation. J. Exp. Med. 172, 497–507.
Rennels, M.L., Gregory, T.F., Blaumanis, O.R., Fujimoto, K., Grady, P.A., 1985. Evidence for a 'paravascular' fluid circulation in the mammalian central nervous system, provided by the rapid distribution of tracer protein throughout the brain from the subarachnoid space. Brain Res. 326, 47–63.
Rollins, B.J., 1996. Monocyte chemoattractant protein 1: a potential regulator of monocyte recruitment in inflammatory disease. Mol. Med. Today 2, 198–204.
Rollins, B.J., Yoshimura, T., Leonard, E.J., Pober, J.S., 1990. Cytokine-activated human endothelial cells synthesize and secrete a monocyte chemoattractant, MCP-1/JE. Am. J. Pathol. 136, 1229–1233.
Rothwell, N.J., 1991. Functions and mechanisms of interleukin 1 in the brain. Trends Pharmacol. Sci. 12, 430–436.
Staykova, M., Maxwell, L., Willenborg, D., 2000. Kinetics and polarization of the membrane expression of cytokine-induced ICAM-1 on rat brain endothelial cells. J. Neuropathol. Exp. Neurol. 59, 120–128.
Stern, E.L., Quan, N., Proescholdt, M.G., Herkenham, M., 2000. Spatiotemporal induction patterns of cytokine and related immune signal molecule mRNAs in response to intrastriatal injection of lipopolysaccharide. J. Neuroimmunol. 106, 114–129.
Stoodley, M.A., Jones, N.R., Brown, C.J., 1996. Evidence for rapid fluid flow from the subarachnoid space into the spinal cord central canal in the rat. Brain Res. 707, 155–164.
Tang, T., Frenette, P.S., Hynes, R.O., Wagner, D.D., Mayadas, T.N., 1996. Cytokine-induced meningitis is dramatically attenuated in mice deficient in endothelial selectins. J. Clin. Invest. 97, 2485–2490.
Thibeault, I., Laflamme, N., Rivest, S., 2001. Regulation of the gene encoding the monocyte chemoattractant protein 1 (MCP-1) in the mouse and rat brain in response to circulating LPS and proinflammatory cytokines. J. Comp. Neurol. 434, 461–477.
Touzani, O., Boutin, H., Chuquet, J., Rothwell, N., 1999. Potential mechanisms of interleukin-1 involvement in cerebral ischaemia. J. Neuroimmunol. 100, 203–215.
Van Dam, A.-M., Bauer, J., Tilders, F.J., Berkenbosch, F., 1995. Endotoxin-induced appearance of immunoreactive interleukin-1β in ramified microglia in rat brain: a light and electron microscopic study. Neuroscience 65, 815–826.
Wong, M.L., Rettori, V., al-Shekhlee, A., Bongiorno, P.B., Canteros, G., McCann, S.M., Gold, P.W., Licinio, J., 1996. Inducible nitric oxide synthase gene expression in the brain during systemic inflammation. Nat. Med. 2, 581–584.

(*Accepted* 28 *January* 2002)